Solvation Ultrafast Dynamics of Reactions. 14. Molecular Dynamics and ab Initio Studies of Charge-Transfer Reactions of Iodine in Benzene Clusters

Julius T. Su and Ahmed H. Zewail*

Laboratory for Molecular Sciences (LMS), Arthur Amos Noyes Laboratory for Chemical Physics, California Institute of Technology, Pasadena, California 91125

Received: December 18, 1997; In Final Form: January 26, 1998

Previous experiments have been carried out in this laboratory to investigate the dynamics of iodine−benzene charge-transfer reactions. Both 1:1 solute−solvent complexes and 1:*n* clusters were studied on the femtosecond time scale with kinetic energy time-of-flight mass spectrometry (Cheng, P. Y.; Zhong, D.; Zewail, A. H. *J. Chem. Phys*. 1996, *105,* 6216). Here, we report theoretical studies of the structure and dynamics of iodine−benzene clusters with direct comparison to experimental findings. In particular, ab initio calculations confirm that iodine binds to benzene near-axially with an energy of 3.5 kcal/mol (MP2/6-311G**), which is consistent with the experimental time scale of the reaction and with the angular and kinetic energy distributions of product fragments. Experimental observations have shown that the dynamics of iodine dissociation under cluster solvation is described by two caging time scales. Using Monte Carlo and molecular dynamics simulations, we find that this effect arises from a fundamental asymmetry in the structure of 1:*n* iodine−benzene clusters. The benzenes tend to form mouth-shaped structures around the iodine, causing one of the iodine atoms to be more strongly solvated than the other. The dynamics therefore reflect two types of solvation forces, free and bound, in a homogeneous structure, rather than a distribution of structures. The two distinct time scales, femtosecond and picosecond, are a result of caging dynamics in the solvent structure. In this way, caging dynamics may be used as a probe of structural features of solvation.

Introduction

When benzene and iodine are brought together to form a complex, an electronic absorption not present in the spectra of either molecule is created, causing a change in the color of their solutions. Mulliken[1] postulated that this band corresponded to electronic transitions from occupied molecular orbitals of benzene to the LUMO of iodine. Known as the charge-transfer (CT) band, it is a dramatically visible consequence of the ease with which iodine may accept an electron from benzene.

Since this charge transfer peak may be readily excited in a selective manner, the iodine−benzene complex has become a useful prototype system for studying the dynamics of charge-transfer reactions. A wealth of studies has been devoted to studying this system in the solution phase; a review of the work can be found in recent publications from Wiersma's group[2] and from this laboratory[3].

Cheng et al.[4] has carried out femtosecond time scale pump−probe experiments on the iodine−benzene and related charge-transfer complexes in a molecular beam. In these experiments, 1:1 and 1:*n* iodine−benzene (fs) complexes were made and identified by mass spectrometry. Then, a femtosecond (fs) laser pulse was used to coherently excite the complexes to their charge-separated state. After such an excitation, the iodine molecules in the complex dissociate on a well-defined time scale. The products from this reaction were monitored via ionization with a second femtosecond pulse.

For the 1:1 species, both the initial iodine−benzene complex and the product iodine atoms were detected; for the clusters, the product iodine atoms were detected, as was necessary to probe the dynamics of iodine atom caging. By resolving velocity distributions and the angular anisotropy of the complex with time, two channels of the reaction were established: one originating from the charge separated state $Bz^+I_2^-$, with I_2^- breaking to produce I atoms in 1.4 ps, and the second from the back electron-transfer process, which produces I atoms in 0.4 ps.

By varying the conditions of the molecular beam, it was possible to vary the size distribution and composition of the iodine−benzene clusters. In this way, the microscopic solvation dynamics of iodine−benzene clusters could be studied. In general, as more benzenes were placed around each iodine molecule, it took longer and longer for released iodine atoms to escape from the benzene "cage". Additionally, two distinct groups of iodine atoms, distinguished by their caging time scale and their velocities, were detected.

This paper describes a molecular dynamics model that has been developed to reproduce these experimental observations from "first principles". Briefly, ab initio calculations were used to find the binding energies and structures of selected 1:1 iodine−benzene complex geometries. Then, an atom−atom potential incorporating electrostatic, dispersive, and repulsive forces was fitted to the ab initio results. The simplified potential, in conjunction with Monte Carlo simulations, was used to find minimum energy and low-temperature configurations of larger iodine−benzene clusters. The iodine molecules in these clusters were then dissociated, and molecular dynamics runs were carried out to simulate the caging dynamics of the "hot" iodine atoms released.

This model ultimately relates structural features of the complex to observed dynamics and addresses a general phenomenon observed in this and other systems,[5] namely the two distinct time scales (fs and ps) involved in solvation dynamics. The structure of this paper follows the development of the

S1089-5639(98)00572-6 CCC: $15.00
Published on Web 04/17/1998

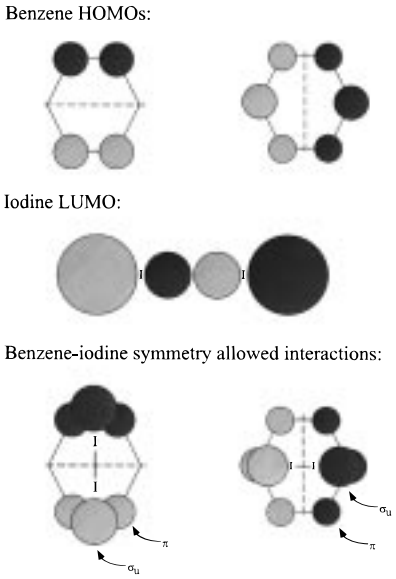

Figure 1. Symmetry-determined iodine and benzene orbitals. The resting iodine structure was originally thought to be favored by considerations of the symmetry of the benzene HOMO−iodine LUMO interaction.

model: first, the theory used to describe the 1:1 iodine−benzene complex is given; then, its extension to the 1:*n* complex is detailed; and finally, the dynamics of iodine dissociation in the benzene clusters is presented.

The Methodology

Preliminaries: 1:1 Complex Structure and Energy. Mulliken considered the wave function of the iodine−benzene complex to be a combination of no-bond and dative (charge separated) wave functions:

$$\Psi(Bz\cdots I_2) = a\Psi_0(Bz, I_2) + b\Psi_1(Bz^+ - I_2^-) \qquad (1)$$

The overall energy of the complex may then be approximated by taking the no-bond complex energy and adding to it an additional charge-transfer stabilization. This stabilization is greatest when the no-bond and dative complexes are similar in energy, and when a resonance parameter β related to the overlap of the corresponding wave functions is large.

From a consideration of symmetry and energies, Mulliken concluded that in a 1:1 iodine−benzene complex, iodine would most probably assume a *resting* configuration, one with iodine lying parallel to the benzene plane with its center on the 6-fold axis of benzene. In reaching this conclusion, he assumed that the most significant contribution to the charge-transfer energy would come from the excitation of an electron from the HOMO of benzene to the LUMO of iodine.

To overlap with each other and make a contribution to the charge transfer energy, the benzene HOMO and iodine LUMO must be oriented so that they are of the same symmetry species. Resting orientations, as shown in Figure 1, clearly satisfy this requirement. Additionally, iodine may be oriented at a oblique angle to benzene, which reduces the symmetry of both species enough to satisfy the requirement. An axial geometry (iodine on the 6-fold axis of benzene) stabilized by a HOMO−LUMO charge transfer is however ruled out on the basis of symmetry. Out of these geometries, the resting structure appears to enjoy the greatest charge-transfer stabilization, since its compactness minimizes the extent of charge separation.

However, Collin and D'Or observed[6] that in chlorine−benzene complexes the Cl_2 stretching frequency was infrared active at 526 cm^{-1}. Similar observations for iodine−benzene complexes were later made by Yarwood and Person.[7] This indicated that chlorine could not be resting symmetrically on the benzene plane. The absorption peak was also particularly broad, leading Collin and D'Or to speculate that the orientation or position of chlorine with respect to benzene was highly variable. On the basis of these data, Mulliken suggested[8] that chlorine would likely be located in an "oblique", tilted away from the benzene plane, or "unsymmetric resting", center shifted away from the 6-fold axis, configuration. He further noted that these new configurations might be favored on the basis of additional dative wave function contributions or a not easily understood variation of the resonance parameter β of the dative wave function with orientation.

Shortly after Collin and D'Or published their results, Ferguson[9] observed that adding either bromine or iodine to a benzene solution caused distinct changes in the infrared spectrum of benzene; specifically, bands at 850 cm^{-1} (an inactive E_{1g} fundamental of benzene) and 922 cm^{-1} (assumed to be an inactive A_{1g} fundamental of benzene) were greatly enhanced; no other enhancement of bands was observed. The enhancement of these bands suggested that the complexed benzene had been symmetry lowered from D_{6h} to C_{6v}. Ferguson cited these results as strong evidence in favor of the axial model. Fredin and Nelander[10] later carried out similar investigations using nitrogen matrixes containing benzene and iodine, where the 1:1 complex was known to dominate. They also observed the selective activation of the E_{1g} and A_{1g} benzene fundamentals.

Finally, Hassel and Stromme carried out X-ray studies of chlorine−benzene[11] and bromine−benzene[12] crystals. Both of the obtained structures showed alternating chains of benzene and axial halogen molecules. For the bromine−benzene complex, it was additionally noted that the X-ray data suggested that the binding forces between the two components were rather weak, and that in fact particularly large amplitude vibrations were present in a direction perpendicular to the 6-fold axis of the benzenes. Hence, the axial model was not absolutely confirmed—it was suggested that the bromine molecules might move between unsymmetric but shallow minima.

In their published text on molecular complexes, Mulliken and Person[13] addressed the experimental evidence for an axial complex and described what further considerations could be made to rationalize a tightly bound axial structure. The axial complex might be stabilized by charge transfer through the removal of an electron from the *lowest* energy π molecular orbital; the larger energy difference could be compensated for by a correspondingly larger resonance parameter β. Additionally, electrostatics and exchange repulsion appeared to favor the axial complex, so that, even if charge-transfer stabilization favored the resting complex, it might be overshadowed by the energetics of the no-bond wave function.

They concluded by noting that the oblique model still appeared reasonable—an oblique structure could enjoy the benefits of better electrostatics and exchange repulsion while still being stabilized by charge transfer: with the complex's low symmetry, electrons from all the benzene π orbitals could participate in charge transfer. Given that the complex is so weakly bound, Mulliken noted, the iodine in its oblique configuration could well be highly mobile in the complex.

Subsequent attempts to develop a better theoretical model to describe halogen-benzene complexes focused on evaluating the relative contributions of electrostatic and exchange repulsion

energies to the binding energy of the complex. Lippert, Hanna, and Trotter[14] used atomic charges, point quadrupoles, and bond polarizabilities to approximate the charge distribution of various aromatic compounds and halogens; from this they calculated Coulomb, induction, and dispersion contributions to the complex's binding energy. Charge-transfer and exchange repulsion energies were calculated using a semiempirical expression for the overlap between pairs of atomic orbitals.

Cook and Schug[15] carried out similar calculations; the main differences arose in how they evaluated the Coulomb energy—through numerical integration over charge distributions of Slater-type orbitals—and how they evaluated exchange repulsion—by calculating the energies of SCF molecular orbitals. Both groups concluded that all interactions examined were of similar enough magnitude that the structure and energy of halogen−benzene complexes could only be understood through a careful consideration of all interactions. In particular, quadrupole-induced dipole and quadrupole−quadrupole interactions proved to be more significant than expected.

Interestingly enough, the role of charge transfer stabilization was considered comparatively small. Lippert et al noted that the charge transfer energy had roughly the same overlap dependence as the exchange repulsion energy; thus, a geometry stabilized by charge transfer would be correspondingly destabilized by exchange repulsion. Cook and Schug's calculations showed that the charge-transfer stabilization of chlorine−benzene complexes was negligible at equilibrium distances.

Schug and Dyson[16] later used the formulation of Lippert et al (preferred over Cook and Schug due to its simplicity) to evaluate the energy of the iodine−benzene complex as a function of iodine orientation and displacement along different axes of benzene. When they constrained iodine to move along the 6-fold axis of benzene, they found the resting structure to be hardly bound at all (−0.03 kcal/mol), the axial structure to be only somewhat more stable (−0.30 kcal/mol); and an oblique structure to be of only intermediate stability (−0.12 kcal/mol). Investigating further, they found one structure, a resting structure centered over and parallel to a carbon bond, to be the most stable of all (−0.31 kcal/mol) due to an extra polarization stabilization effect.

The next series of theoretical models, developed almost a decade later, began to use "supermolecule" SCF orbitals to calculate benzene−halogen binding energies. These calculations used fewer empirical parameters, but provided less information than the previous perturbation theory calculations on the relative contributions of different energy components (one is reminded of Mulliken's concern that "... the more accurate the calculations became, the more the concepts tended to vanish into thin air."[17]) In the limit of a complete set of basis functions, for instance, the charge-transfer interaction between two molecules is included in the induction energies of the individual molecules, making the inclusion of a charge-transfer term spurious.[18]

Using the CNDO/2 method, Schug and Levinson[19] found minimum energy structures of the chlorine−benzene complex that satisfied certain geometrical constraints. They found structures where the center of chlorine was placed on the 6-fold axis to be particularly unstable (the most stable configuration, an oblique structure tilted about 20° away from the 6-fold axis, had an interaction energy of −0.60 kcal/mol). More encouraging results were obtained by fixing chlorine above a carbon atom of benzene; the most stable resulting configuration, an oblique structure tilted 30° away from the 6-fold axis, had an interaction energy of −3.53 kcal/mol.

Bruns,[20] using a larger basis set, extended the CNDO/2 work of Schug and Levinson to include two additional complex geometries, where an axially oriented chlorine molecule was placed above both carbon atoms and carbon−carbon bonds of benzene. All of his calculated binding energies were significantly larger than previously obtained experimental or theoretical results; his most stable structure, consisting of an axial chlorine above a carbon−carbon bond, had a binding energy of −19.2 kcal/mol at an equilibrium distance (from here on, measured center to center) of 3.01 Å.

Jano[21] carried out INDO calculations to find the minimum energy geometries of axial and resting configurations of the iodine−benzene complex. In both cases, the center of iodine was restricted to lie on the 6-fold axis of benzene. He found both geometry types to have an equilibrium separation of about 3.9 Å; however, the resting structure had a negligibly small binding energy (−0.06 kcal/mol), while the axial structure had quite a substantial binding energy (−18.1 kcal/mol).

It has been possible to carry out ab initio calculations on benzene−halogen and related complexes. Lucchese and Schaefer[22] made such calculations using an STO-3G basis set representation to calculate the energy of chlorine−benzene and flourine−benzene complexes at the Hartree−Fock level of theory. They found the equilibrium axial structures of these complexes to be very weakly bound (0.03 and 0.06 kcal/mol) and so did not pursue the calculations further. Kochanski and Prissette[23] carried out a more complete set of calculations on the chlorine−benzene and iodine−benzene complexes. The total energy of the complex was evaluated as a sum of SCF and dispersive energies; the component energies were calculated using separate sets of basis functions.

For the SCF calculation, unpolarized basis functions for the two highest energy shells of hydrogen, carbon, and iodine were contracted into double-ζ basis sets; the inner shells were represented with a single-ζ basis set. For the dispersive energy calculations, the primitive functions were recontracted to a single-ζ basis set and diffuse functions were added to each atom. The basis set superposition error (BSSE) for all complex geometries was determined and corrected. Iodine was constrained to be lying axially either above the center of benzene or above a carbon−carbon bond of benene; the latter geometry was termed the perpendicular-to-bond geometry (PB). The equilibrium C_6-centered geometry with an energy of −1.94 kcal/mol was only slightly more stable than the above-bond geometry with an energy of −1.87 kcal/mol.

More recently, Wiersma's group[24] and this laboratory have independently carried out ab initio calculations on the iodine−benzene complex. The difference in techniques used and results obtained will be discussed in detail in the forthcoming sections. Following Schug and Dyson,[16] we have considered both symmetric and asymmetric axial, oblique, and resting structures. Our calculations have been carried out at a high level of theory using a fairly complete yet reasonably sized basis set.

Our results indicate that, in order of decreasing magnitude, axial structures are more stable than resting structures; uncentered structures are more stable than centered structures; and bond-centered structures and carbon-centered structures are equally stable. The energy differences corresponding to these structural differences average to roughly 2, 0.3, and <0.005 kcal/mol, respectively. The lowest energy structure obtained was an axial oblique uncentered structure with an energy of −3.5 kcal/mol. Bond-centered and carbon-centered forms of this structure had identical energies.

Ab Initio Calculations: the 1:1 Complex. Theoretical studies have indicated that the contribution of the charge transfer interaction to the stability of charge transfer complexes has been systematically overestimated. Indeed, the geometries of many such complexes may be explained only through a careful consideration of electrostatic, dispersive, and polarizability interactions. For the iodine−benzene complex, these interactions are of similar enough magnitude that the structure of the complex may not be readily predicted on the basis of a single, well-understood interaction. Ab initio calculations have therefore been carried out on the iodine−benzene complex in order to more directly model the subtle interplay of these electronic interactions.

When the energy of a iodine−benzene complex was determined, the entire complex was taken to be a single supermolecule. The restricted Hartree−Fock energies of the iodine molecule−benzene complexes and the unrestricted Hartree−Fock energies of the iodine atom−benzene complexes were then calculated. The SCF binding energy was determined by subtracting the energy of the complex from the energy of a complex with a iodine−benzene separation distance of 10 angstroms. Electron correlation effects were subsequently included by adding Moller−Plesset perturbative corrections to the second order (MP2) to both complex energies. Additionally, counterpoise corrections were applied to the optimized geometries to determine the extent of basis set superposition error (BSSE).

A 6-311G** basis set was used to represent the hydrogen and carbon atoms. The iodine atoms were represented by the HW3 basis set developed by Danovich, Hrusak, and Shaik.[25] The HW3 basis set is a double-ζ valence electron basis set with a Hay−Wadt pseudopotential and two additional uncontracted d-type polarization functions added. Hay−Wadt pseudopotential basis sets for iodine have been widely used to model both iodine-containing molecules and iodine-containing complexes.[26−29]

Minimum energy and transition state geometries of iodine bound to benzene were found using noncounterpoise corrected energies and Gaussian 92's[30] geometry optimization routine. In this process, the molecules' bond lengths were optimized and fixed before the complex was formed. This restriction made it possible to fit the ab initio energies to the rigid molecule atom−atom potential used for larger complexes. Once the molecules were placed together, they were allowed to move freely relative to each other with one constraint: in complexes containing I_2, the projection of the iodine bond onto benzene was required to stay on a single line passing through the center of benzene. Within this constraint, the position of an iodine atom relative to benzene may be specified by two variable coordinates, namely the projection of the atom's position parallel and perpendicular to benzene's C_6 axis. The description of the I_2−benzene geometry requires that the angle between the iodine bond and the C_6 axis of benzene be specified as well. A summary of the coordinate system used for I_2−benzene is shown in Figure 2.

Three sets of calculations were carried out to search for stationary points along the iodine−benzene complex potential energy surface (PES). As it turns out, both I and I_2 may move around the benzene ring with little change in energy, making the corresponding PES coordinate particularly shallow. This near-cylindrical symmetry of benzene from iodine's perspective made it desirable to constrain the motion of iodine to certain planes, described as either carbon-centered or bond-centered, passing through benzene's C_6 axis. The iodine may also be constrained to move at the intersection of the two planes, the C_6 axis of benzene.

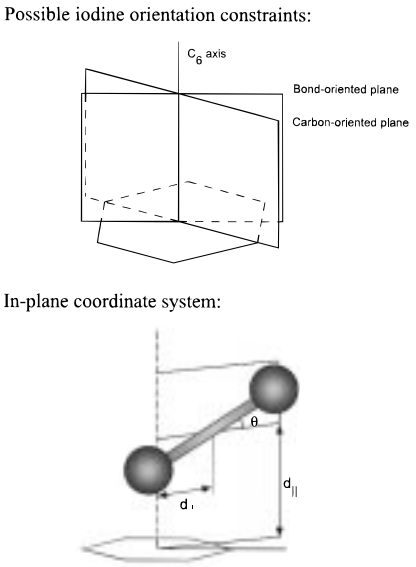

Figure 2. Iodine-benzene coordinates are specified by an iodine orientation constraint and an in-plane set of coordinates.

Both the I-benzene and axial or resting I_2-benzene geometries are therefore classified as carbon-centered, bond-centered, or C_6 axis-centered geometries, depending on which plane the iodine occupies. Although there are no restrictions on the position of iodine within these planes, it happens that the iodine in carbon-centered structures tends to lie above a carbon atom, while the iodine in bond-centered structures tends to lie above a carbon−carbon bond.

Once optimized, these geometries were classified as minima or transition states by calculating the non-BSSE corrected energies of similar geometries in the constraining plane and comparing them to the energy of the original geometry. This procedure also allowed us to estimate the force constants corresponding to the relative motions of the complex molecules within the constraining plane, and with certain approximations, the zero-point energy contributions to the complex binding energies.

Finally, we checked the quality of our benzene basis set by calculating the energies of the 6-311G** optimized geometries with a 6-31+G* basis set, reasoning that any deficiency in our basis set would likely arise from a lack of diffuse functions on benzene. The results, included along with the 6-311G** energies shown in Table 1, show that the energy differences are small, averaging near 10% for transition state geometries and 5% for minimum energy geometries. Reoptimizing C_6 axis-centered I_2-benzene geometries with a 6-31+G* basis set produced only slight changes in I_2−Bz distances (from 4.775 to 4.803 Å for the axial structure, and from 3.930 to 3.881 Å for the resting structure). We therefore conclude that our 6-311G** energies as shown are good and may be used to obtain a reasonable atom−atom potential.

Atom−Atom Potential for 1:*n* Clusters. To model the dynamics of larger complexes, we have derived a simple atom−atom potential that may be used to represent interactions between iodine and benzene. One interaction site was placed on each atom in benzene, one interaction site was placed on each separated iodine atom, and three interaction sites were placed on each iodine atom that was bound into a molecule. Interactions between pairs of sites were taken to be the sum of repulsive, dispersive, and electrostatic interactions:

TABLE 1: Intermolecular Energies (kcal/mol) of Iodine Molecule−Benzene and Iodine Atom−Benzene Minimum Energy (Carbon, Bond Centered) and Transition State Geometries (C_6 Centered)

geometry	SCF binding energy	MP2 correction	BSSE correction	total energy (6-311G**)	total energy (6-31+G*)
I_2 axial C_6 centered	0.706	−5.920	1.873	−3.340	−2.948
I_2 axial C_6 centered (tilted)	1.433	−6.839	2.183	−3.222	−2.887
I_2 axial carbon centered	1.538	−7.888	2.852	−3.498	−3.281
I_2 axial bond centered	1.633	−7.981	2.850	−3.498	−3.270
I_2 resting C_6 centered, bond oriented	2.590	−5.008	1.294	−1.124	−1.023
I_2 resting C_6 centered, carbon oriented	2.574	−4.984	1.284	−1.126	−1.024
I_2 resting bond centered	2.512	−5.918	1.713	−1.694	−1.613
I_2 resting carbon centered	2.475	−5.830	1.682	−1.672	−1.602
I atom C_6 centered	0.705	−4.187	1.306	−2.176	−1.941
I atom bond centered	2.167	−6.675	2.232	−2.276	−2.305
I atom carbon centered	1.256	−5.393	1.740	−2.398	−2.305

[a] All energies calculated using 6-311G** for hydrogen and carbon and HW3 for iodine unless otherwise indicated.

$$U = \sum_i \sum_{j<i} A_{ij} e^{-B_{ij} r_{ij}} - \frac{C_{ij}}{r_{ij}^6} + \frac{q_i q_j}{r_{ij}} \qquad (2)$$

Each molecule was assumed to be a rigid body; hence, the interaction sites in each body were kept fixed relative to each other. Multiple charge centers were used to model higher order electrostatic moments (i.e., the quadrupoles of benzene and iodine).

The standard Williams potential with short (1.027 Å) carbon−hydrogen bonds was used to model benzene−benzene interactions. In this potential, the electrostatics of benzene are modeled with equal and opposite point-charges ($q_{C/H} = \pm 0.115e$) placed on the carbon (+) and hydrogen (−) atoms. The electrostatics of the iodine molecule was modeled by placing six point-charges along the iodine bond with a location and strength chosen to match the ab initio electrostatic potential of iodine around selected isodensity contours ($q_i = +0.83e, -2 \times 0.83e, +0.83e$ with the negative charge at the atom center and the positive charges by 0.7 Å on each side, representing the quadrupole on each I atom). A diagram showing the point-charges used and the resulting electrostatic potential surface is shown in Figure 3. Note that the significant differences in electrostatic potential are contained within the core of the iodine molecule, where benzene molecules are not expected to penetrate.

The first isodensity contour around iodine contains roughly 99% of the molecule's electron density; the second contour is not actually an isodensity contour, but is simply the first contour scaled in all directions by a factor of 1.5. The strength and location of the point-charges were derived by assuming initially that the charge distribution along the iodine bond was composed of "basis functions." Then, the electrostatic potential of different sets of basis functions, including sinusoidal and Gaussian charge distributions, was calculated; the basis function potentials were orthonormalized; the overlap between the given electrostatic potential and that of each basis function was determined; and from this the correct linear combination of basis functions was derived.

Nonelectrostatic interactions between iodine atoms and other atoms were assumed to take place only between actual atom positions. The parameters describing these interactions were selected to approximately reproduce the binding energies and geometries of C_6-centered iodine molecule−benzene and iodine atom−benzene structures. Only the iodine−iodine interaction parameters were specifically varied; combination rules were used to derive the other parameters. The resulting potential, using parameters given in Table 2, reproduced the binding energies and molecule separation distance of the selected geometries to within 0.1 kcal/mol and 0.1 Å, respectively.

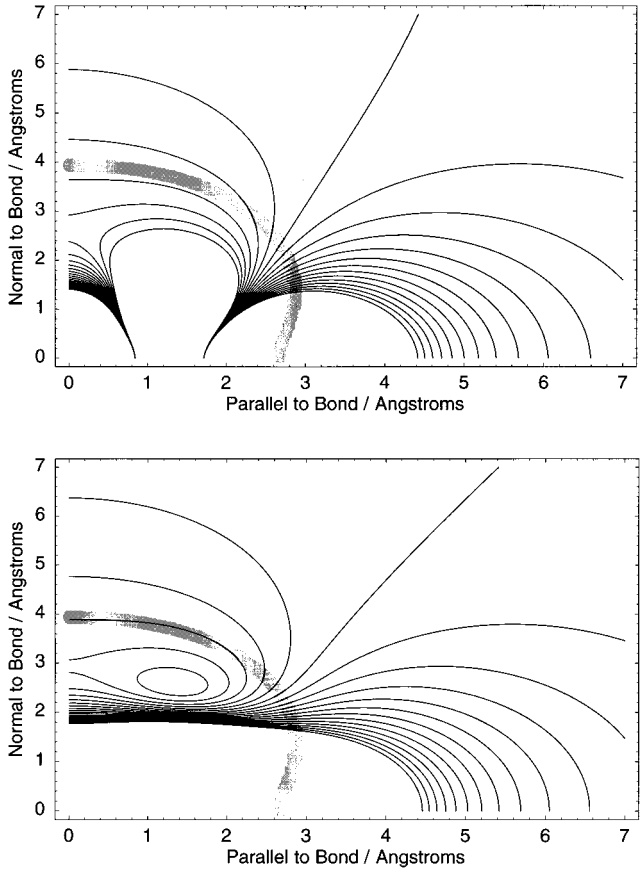

Figure 3. Point charge description of iodine (top) and its associated electrostatic potential compared to the ab initio derived potential (bottom). The heavy gray line is an isodensity contour containing roughly 99% of iodine's electron density.

The dissociation of iodine was modeled by replacing the rigid iodine molecule by two separate iodine atoms that interact via a repulsive exponential potential, as described in Cheng et al.[4] When this happened, a different set of van der Waals parameters was used to describe the interactions of these free iodine atoms with benzene. This change of parameters is intended to reproduce, in an average way, the electrostatic interaction between the iodine atoms and benzene that can no longer be explicitly described once the iodine atoms are considered as separate point bodies.

Minimum Energy 1:*n* Clusters. Using the atom−atom potentials derived above, we attempted to find the absolute minimum energy geometry of several iodine−benzene clusters. To do this, Monte Carlo simulations were carried out at a temperature high enough to "melt" the clusters and sample a

TABLE 2: Potential Parameters Used in the Simulation (before and after Dissociation)

	A (kJ mol^{-1} Å^6)	B (kJ mol^{-1})	C (Å^{-1})
	Before Dissociation		
H−H	136.4	11 971.0	3.74
H−C	576.9	66 529.6	3.67
H−I	1252.0	86 702.9	3.44
C−C	2439.0	369 743.0	3.68
C−I	5295.3	481 857.5	3.37
I−I	11492.8	627 967.6	3.14
	After Dissociation		
H−H	136.4	11 971.0	3.74
H−C	576.9	66 529.6	3.67
H−I	1715.8	179 637.2	3.67
C−C	2439.0	369 743.0	3.68
C−I	7256.8	998 346.0	3.60
I−I	0.0	28 942.6	2.00

large portion of configuration space; at regular intervals, the geometries obtained were "quenched" using a conjugate gradient optimization method.

For each series of runs, we began with a previously obtained 1:(n − 1) iodine−benzene absolute minimum energy structure. A single benzene molecule was then added to the cluster at an arbitrary location, generally selected to be near the iodine molecule on a side opposite to the other benzenes. The 1:(n − 1) cluster was frozen, and the added benzene was allowed to move around to a local energy minimum via direct energy minimization. Then the entire complex was heated to a temperature of 200 K for 2000 trial moves.

At each trial move, all of the molecules in the cluster were moved at once. Quaternions were used to represent the orientation of each molecule; a random rotation thus consisted of a random step on the quaternion parameter four-sphere. The maximum allowable rotation and translation steps were kept at the fixed ratio of 0.01 (quaternion parameter/angstrom). The acceptance ratio was kept near 0.5 by varying the step size of the trial moves during the simulation.

After heating, the clusters were immediately cooled to 30 K for 10 000 trial moves. The resulting cluster was then quenched to a local energy minimum, the structure was stored, and the cluster was heated to 200 K again. The lowest energy structure of out of 10 such runs was then taken as the absolute minimum energy structure. This structure was then used as the starting point for the construction of clusters with additional benzenes.

Molecular Dynamics and Iodine Dissociation in 1:*n* Clusters. In simulating the dissociation of iodine in benzene clusters, we attempted to obtain an ensemble of starting configurations that would be representative of the distribution of clusters inside a molecular beam. To do this, the absolute minimum energy clusters obtained previously were "melted" (200 K for 2000 trial moves) and then cooled to the expected vibrational temperature of the molecular beam (30 K for 10 000 trial moves) using the Monte Carlo procedures described above. All of the clusters in the ensemble were then given rotational velocities corresponding to an overall Boltzmann distribution of rotational energy; this distribution was selected to match the expected rotational temperature of the molecular beam, 10 K. The translational energy distribution of the clusters was assumed to be irrelevant.

Molecular dynamics runs were then carried out. For these runs, all of the molecules were assumed to be rigid and were represented using the quaternion formalism. The leapfrog scheme of Potter[31] was used to integrate the translational and rotational equations of motion with a fixed time step of 2 fs.

Each initial configuration, starting only with some rotational velocity, was equilibrated for 10 ps to allow its energy components to be redistributed. The variation in kinetic energy over the course of the run turns out to be comparable to the kinetic energy itself, so the system does not need to evolve far, usually less than 1 ps, to be considered equilibrated. Following this, and marking time zero, the iodine molecule was changed from a single rigid body to two separate atoms, and the atom−atom potential was switched to a dissociative potential. The dissociative run was then carried out for 50 ps. One hundred equilibration and dissociative trajectories were calculated for 1:1, 1:2, 1:5, and 1:10 iodine−benzene clusters. The root-mean-square (rms) variation in total energy over all trajectories was typically less than one part in 10^4 for dissociative runs and less than one part in 10^5 for equilibration runs.

It is important to remember that in our dynamics simulation, it has been assumed that the excitation of the complex to its charge transfer state is *immediately* followed by coupling to a neutral iodine repulsive state. The dynamics of the charge-separated form of the complex are thus neglected.

Results and Discussion

Ab Initio Calculations. A total of eight minimum energy iodine molecule−benzene geometries and three minimum energy iodine atom−benzene geometries were determined. Each of these geometries were optimized with different constraints. In particular, axial and resting iodine molecule/atom−benzene geometries centered over the C_6 axis, carbon atoms, and carbon−carbon bonds of benzene were examined. The energies and structural parameters of these geometries are given in Tables 1 and 3. Figure 4a shows the axial C_6-centered structure that has traditionally been taken to be the minimum energy structure of the complex. Our calculations indicate that this structure is actually a transition state of the complex, and that the axial and resting structures shown in Figure 4b and c are more representative of the energy minima associated with the complex.

It should be noted that the two axial C_6-centered geometries shown in the table differ in that the iodine of the first geometry is constrained to lie along the C_6 axis of benzene, while in the second geometry, no such constraint is present. The *uncorrected* energy of the tilted-iodine complex is lower than the energy of the vertical-iodine complex; however, when the BSSE correction is applied, the energy of the vertical-iodine complex is shown to be lower. Since the difference in energies is within the error of the calculation, no conclusion can be drawn about the preferred orientation of iodine held over the center of benzene.

As mentioned in the Introduction, the structures may be placed into a hierarchy of binding energies. All of the axial structures considered were more stable than the resting structures; all of the uncentered structures were more stable than the centered structures; and the bond-centered structures and carbon-centered structures had roughly the same energy. As a consequence of this, the movement of iodine around the benzene ring is unrestricted, and the movement of iodine across the plane of benzene is hindered by an energy barrier of only 0.3−0.4 kcal/mol. However, any rocking motion of the iodine molecule is restricted, since the axial form of the complex is more stable than the resting form by roughly 2 kcal/mol. These results are schematically illustrated in Figure 5.

Small displacements of iodine relative to benzene were made relative to axial and resting structures to obtain force constants corresponding to intermolecular degrees of freedom. If it is assumed that the change in vibrational frequencies of the individual iodine and benzene molecules is small relative to the vibrational frequencies derived from these new degrees of freedom, the zero-point energy contribution to the binding

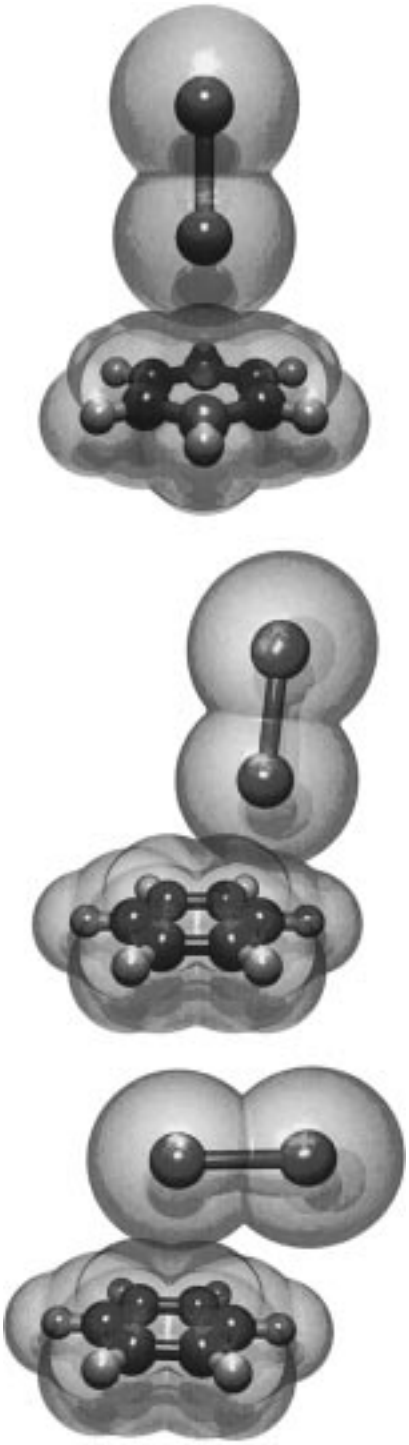

Figure 4. Representative ab initio geometries: (a) axial C_6-constrained geometry, representing a transition state of the complex, (b) axial carbon-centered geometry, representing one of the complex's absolute energy minima, (c) resting carbon-centered geometry, representing another set of energy minima.

energy of the complex may be found from these force constants, as shown in Table 4. As expected, the force constant corresponding to motion perpendicular to the C_6 axis across the plane of benzene is relatively small compared to the other force constants. We see that the zero-point energy contribution weakens the binding of the axial and resting complexes by about 0.55 and 0.36 kcal/mol, respectively. In contrast, Yarwood and Person's far-IR measurements[7] showed that iodine's vibrational frequency upon binding benzene shifted from 213 to 205 cm^{-1}, corresponding to a zero-point energy shift of 0.02 kcal/mol and

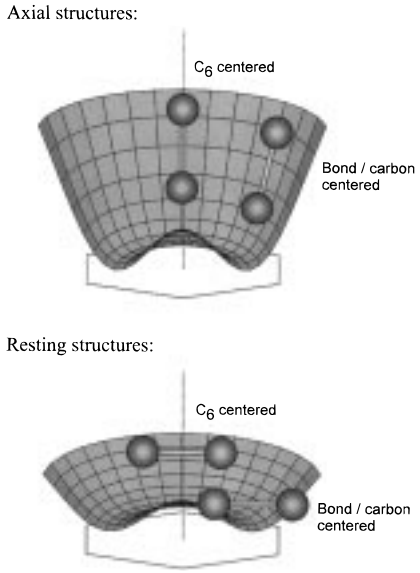

Figure 5. Schematic potential energy surfaces describing the relative energies of the ab initio geometries. Note that the C_6 axis constrained geometries correspond to the complex's transition states.

making our approximation a reasonable one. The approximate nature of this zero-point energy estimate precludes us from formally adding its contribution to the total binding energy of the complex.

The "supermolecule" nature of the ab initio calculation prevents us from decomposing the binding energy into chemically meaningful components. However, we would like to gain a qualitative understanding of the interactions leading to the difference in binding energies observed among the complexes studied. To do so, we consider the SCF binding energy to be the sum of electrostatic, exchange repulsion, and polarizability effect interactions; the MP2 correction to be the dispersive interaction between molecules; and the BSSE correction to be a rough measure of charge-transfer interaction.

This oversimplification (as shown below) leads to the conclusion that the stability of all the complexes are due to dispersive interactions. More significantly, we find that the stability of axial structures over resting structures is primarily due to dispersive interactions (the change in dispersive binding energy $\Delta\Delta E$ between axial and resting structures is ≈ -2 kcal/mol) and electrostatics, exchange repulsion, and polarizability effects ($\Delta\Delta E \approx -1$ kcal/mol). The charge-transfer interactions in the axial structure, though, are weaker by around 0.5 kcal/mol. Additionally, the axial off-centered structures are preferred over axial-centered structures on the basis of dispersive interactions ($\Delta\Delta E \approx -2$ kcal/mol). These favorable interactions are however almost entirely canceled out by the loss of stability from the electrostatic + exchange repulsion + polarizabilty contribution ($\Delta\Delta E \approx +1$ kcal/mol) and from the charge-transfer interaction ($\Delta\Delta E \approx +1$ kcal/mol). The situation is similar for resting structures; resting off-centered structures are stabilized over resting centered structures by stronger dispersive interactions ($\Delta\Delta E \approx -1$ kcal/mol), but this is offset by a loss of charge-transfer stability ($\Delta\Delta E \approx 0.5$ kcal/mol).

Our ab initio structural results, namely, that iodine will tend to form an oblique, highly mobile complex with benzene, are consistent with experimental observations. Collin and D'Or's[6] observation of a halogen dipole moment in bound complexes led Mulliken to propose the oblique structure; the further observation of a particularly broad absorption peak suggested that the position of iodine over benzene was highly variable.

TABLE 3: Geometry Parameters (Distances in Å, Angles in deg) of Iodine Molecule−Benzene and Iodine Atom−Benzene Minimum Energy (Carbon, Bond Centered) and Transition State (C_6 Centered) Geometries

geometry	distance || to C_6 axis	distance ⊥ to C_6 axis	angle away from vertical or horizontal
I_2 axial C_6 centered	4.78	0 (fixed)	0 (fixed)
I_2 axial C_6 centered (tilted)	4.62	0 (fixed)	18.5°
I_2 axial carbon centered	4.48	1.55	5.3°
I_2 axial bond centered	4.47	1.57	5.9°
I_2 resting C_6 centered, bond oriented	3.93	0 (fixed)	0 (fixed)
I_2 resting C_6 centered, carbon oriented	3.93	0 (fixed)	0 (fixed)
I_2 resting bond centered	3.69	1.48	0.5°
I_2 resting carbon centered	3.74	1.43	2.9°
I atom C_6 centered	3.54	0 (fixed)	
I atom bond centered	3.15	1.62	
I atom carbon centered	3.32	1.21	

TABLE 4: Force Constants (in kcal/(mol Å^2) for Displacements and kcal/(mol deg^2) for Rotations) Corresponding to Iodine−Benzene Intermolecular Degrees of Freedom and Their Associated Zero Point Energies (in kcal/mol)

	|| to C_6 axis		⊥ to C_6 axis		θ rotation	
geometry	$k_{\|\|}$	$\hbar\omega_{\|\|}$	$k_\perp$	$\hbar\omega_\perp$	k_θ	$\hbar\omega_\theta$
axial C_6 centered	19.1	0.176	−2.3		-1.9×10^{-3}	
resting C_6 centered	10.4	0.129	−1.4		-4.7×10^{-3}	
axial bond centered	25.2	0.202	5.7	0.096	15.1×10^{-3}	0.253
resting bond centered	11.7	0.138	3.0	0.069	5.7×10^{-3}	0.156

Ferguson,[9] and later Fredlin and Nelander,[10] observed an enhancement of certain infrared bands that would correspond to a lowering in complex symmetry from D_{6h} to C_{6v}. And indeed, our time-averaged structure, through not axial, has C_{6v} symmetry. Finally, Hassel and Stomme's[11] X-ray structures of bromine−benzene crystals suggested that the complex was weakly bound and took an axial form. They observed, as we would expect from our results, that particularly large amplitude vibrations were present in a direction perpendicular to the 6-fold axis of benzene.

On the other hand, our results do not agree well with many previous theoretical calculations. In almost all cases, axial structures were shown to be more stable than resting structures; however, the binding energies and geometries calculated differed significantly from our results. Schug and Dyson,[16] for instance, obtained complex binding energies that were lower than our energies by an order of magnitude. The iodine−benzene separation for their axial complex was close to 7 Å, much larger than our 4.8 Å. Interestingly enough, they found an unusual lowest energy structure − a resting structure with the iodine bond parallel to the carbon−carbon bond of benzene. We did not carry out calculations on this structure.

Schug and Levison[19] carried out calculations on the chlorine−benzene system; we cannot, therefore, compare our binding energies or geometries with theirs. We note, however, that their most stable structure, an oblique noncentered structure, was similar to ours. Jano,[21] who did study iodine−benzene, found an axial structure binding energy almost 5 times greater than ours (his resting structure was barely bound). The iodine−benzene separation for his axial structure was close to 3.9 Å, almost an angstrom shorter than ours.

From these comparisons, we conclude that our results are not in agreement with the older semiempirical calculations carried out on the iodine−benzene complex. This is not unexpected; indeed, the semiempirical calculations themselves, some of which made use of many nonstandard approximations, disagreed with each other substantially.

Kochanski and Prissette[23] carried out ab initio calculations on the iodine−benzene complex. As it turns out, the geometries they obtained were close to our geometries: their axial C_6-centered geometry was separated by 4.77 Å, and ours is separated by 4.78 Å; their axial bond-centered geometry was separated by 4.51 Å, and ours is separated by 4.47 Å. Their axial C_6-centered and bond-centered geometries were less stable than ours by almost 1.4 and 1.6 kcal/mol, respectively.

More recently, Everdij and Wiersma[24] have performed more comprehensive ab initio calculations on the complex. They have carried out their calculations at the MP2 level of theory, using 3-21G basis functions to represent the atoms of benzene and a Hay−Wadt effective core potential to treat the core electrons of iodine.

The description of their results focuses mainly on C_6 centered structures: their axial centered structure is bound by 2.11 kcal/mol and is separated by 5.2 Å, while their resting centered structure is bound by 0.15 kcal/mol and is separated by 4.7 Å. These energies were presented without BSSE correction; with the correction, the axial centered structure is bound by 0.95 kcal/mol. A similar calculation found a carbon-centered axial structure to be bound by 0.98 kcal/mol (corrected) and 1.70 kcal/mol (uncorrected).

In other words, their axial structure is bound less closely than our axial structure by 0.4 Å; their resting structure is bound less closely than our resting structure by 0.8 Å. Energetically, their axial and resting complexes are bound less tightly than our complexes by almost 2 kcal/mol (using their BSSE corrected energy 0.95 kcal/mol) and 1 kcal/mol (using their uncorrected energy 0.15 kcal/mol). Finally, their BSSE corrected axial C_6 centered and axial carbon centered structures are almost identical in energy, suggesting that there is no real energy barrier to iodine moving across the benzene plane.

We conclude that our axial geometries are almost exactly those found by Kochanski and Prissette and are similar to those of Everdij and Wiersma. However, the binding energies found by ourselves, by Kochanski et al., and by Everdij et al. differ in ways most probably associated with the different basis sets used. Everdij and Wiersma used a relatively small set of basis functions to represent benzene with no polarization or diffuse functions; it is therefore likely that they underestimated the dispersion energy of the complex, leading to a low binding energy. We have added polarization functions to both iodine and benzene, and have allowed the carbon and hydrogen atoms of benzene more flexibility through a triple-ζ representation.

Kochanski and Prissette went a step further and carefully tuned their basis functions to the energy components being calculated. For example, when calculating the SCF energy, they represented the two outer shells of carbon and iodine using an unpolarized double-ζ basis set. When calculating the dispersion energy, they lowered the basis set to single-ζ quality and placed added polarization and diffuse functions on all atoms.

TABLE 5: Comparison of 1:1 Complex Heats of Formation (All ab Initio Results Are Given with BSSE Correction)

group	method used	value obtained, kcal/mol
our calculation	ab initio	3.50
	average over configurations (300 K)	1.44
Kochanski and Prissette[23]	ab initio	1.94
Everdij and Wiersma[24]	ab initio	0.95
Jano[21]	INDO	18.1
Danten, Guillot, and Guissani[34]	semiempirical	3.03
	average over configurations (300 K)	2.1
Schug and Dyson[16]	semiempirical	0.31
Atack and Rice[37]	thermodynamic, gas phase (450 K)	2.44
Lang and Strong[38]	spectroscopic, gas phase (300 K)	2.0 ± 0.2
Duerksen and Tamres[39]	spectroscopic, gas phase (300 K)	2.37

Our calculations used a large standard basis set, while Kochanski and Prissette used a smaller basis set specifically adjusted for the system being studied. Despite this, our geometries agree well, although the differences in binding energies remain unexplained. Since entirely different sets of basis functions were used to represent the atoms involved, it is likely to be explicable only in a qualitative sense. Both Chalasinski et al.[32] and Hobza et al.[33] have written reviews of the considerations, particularly in choice of basis set, that must be made when doing ab initio calculations on benzene-containing van der Waals clusters.

A summary of experimentally determined and calculated heats of formation for the iodine−benzene complex is given in Table 5. Where a temperature is not given, the absolute minimum energy of the complex is provided. This is essentially the heat of formation of the complex at absolute zero, and should not be directly compared to heats of formation obtained experimentally at room temperature. Instead, as we describe in the next section, we must calculate the complex's heat of formation as an average over multiple configurations.

Atom−Atom Potential. Our approach in obtaining an isotropic atom−atom potential for the iodine−benzene system is similar to the approach used by Danten, Guillot, and Guissani,[34] who previously studied the dynamics of iodine in benzene solution. In both cases, the standard Williams potential (see ref 34) was used to describe benzene−benzene interactions. A different strategy was used, however, for deriving a potential describing the iodine−benzene interaction. In particular, when deriving a point-charge representation for iodine, Danten et al used four sites, placing two charges on the atom sites and symmetrically displacing the two other charges from the atom sites. The magnitude of the charges and their displacements were constrained to reproduce a quadrupole moment obtained from the ab initio calculations of Straub and McLean[35] ($Q = 18.7 \times 10^{-40}$ C m^2).

We focused on reproducing accurately the close range electrostatic potential of iodine, since in our clusters, the majority of interactions prior to iodine dissociation are short ranged. The six-point-charge representation was chosen after attempting to reproduce iodine's electrostatic potential using different numbers of harmonic, Gaussian, and delta-functionlike basis functions. The fitted charge distributions along the iodine bond resulting from these trials are shown in Figure 6; a summary of the rms error and quadrupole moments of the representations is given in Table 6.

When five basis functions were used, the charge distributions showed a characteristic five-site charge localization, similar to the four-site model used by Danten et al. with an additional site at the bond midpoint. Repeating the fits with 10 basis functions further indicated that the rms error could be reduced by an order of magnitude by using a six site model. The charge

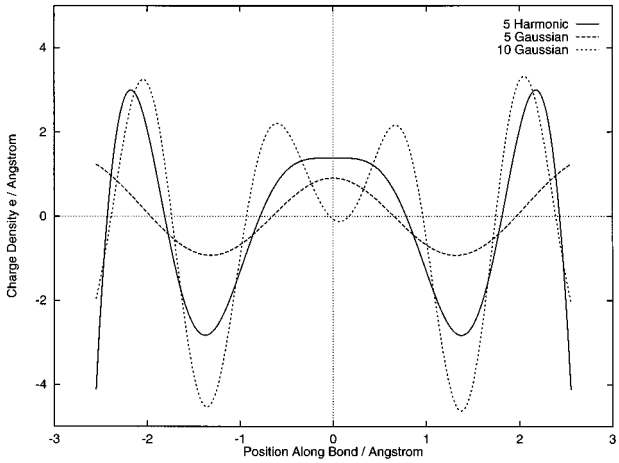

Figure 6. Comparison of iodine bond charge distribution fit using different sets of harmonic and Gaussian basis functions.

TABLE 6: Electrostatic Potential Fits Using Different Sets of Charge Distribution Basis Functions

	rms error (C)	quadrupole moment (10^{-40} C m^2)
5 harmonic	2.271×10^{-7}	54.7
10 harmonic	2.228×10^{-7}	54.7
5 Gaussian	1.731×10^{-6}	52.4
10 Gaussian	2.256×10^{-7}	54.6
5 delta functions	1.974×10^{-6}	52.1
10 delta functions	2.236×10^{-7}	54.7
point charge model	4.139×10^{-7}	52.1

distribution obtained with 10 harmonic basis functions should be disregarded, since the error due to the integration of highly oscillatory functions is likely to be high, and the overlap between the electrostatic potential of two harmonic functions is small.

The six-point charge model has an rms error approximately double that of the 10 basis function representations; this is regarded as adequate for our purposes. As it turns out, the quadrupole moment of this point-charge model, $Q = 52.1 \times 10^{-40}$ C m^2, is quite close to the quadrupole moment obtained from our ab initio calculations, $Q = 56.0 \times 10^{-40}$ C m^2. This indicates that this point-charge model is an accurate representation of the electrostatics of iodine at both short and long ranges. The discrepancy between our ab initio quadrupole moments and that of Straub and McLean is probably due to the inadequacy of the iodine basis set that they used: they had intended to use their iodine basis set to study the properties of halogenated acetylenes, and they were forced to use a single-ζ basis set for iodine so that their four-atom calculations would be computationally feasible.

As in our calculation, Danten et al.[34] used combination rules to derive iodine−benzene interaction parameters from iodine−

TABLE 7: Comparison of Equilibrium Geometries and Binding Energies Obtained with Our Force Field versus That of Danten et al.[34]

	$d_{\|}$ along C_6 (Å)		$d_{\perp}$ to C_6 (Å)		ΔE (kcal/mol)	
geometry	ours	theirs	ours	theirs	ours	theirs
axial C_6 centered	4.86	4.94	0[a]	0[a]	−3.278	−3.034
resting C_6 centered, bond oriented.	3.84	3.82	0[a]	0[a]	−1.218	−2.086
resting C_6 centered, carbon oriented	3.89	3.81	0[a]	0[a]	−1.225	−2.091
resting bond centered	3.65	3.71	1.89	1.77	−1.342	−2.433
resting carbon centered	3.57	3.65	2.05	1.79	−1.377	−2.451

[a] Fixed value.

TABLE 8: Comparison of Energy Components Obtained with Our Force Field versus that of Danten et al.[34]

	ΔE_{elec}		ΔE_{disp}		ΔE_{repl}	
geometry	ours	theirs	ours	theirs	ours	theirs
axial C_6 centered	−2.298	−1.148	−3.022	−3.739	2.042	1.852
resting C_6 centered, bond oriented.	0.649	0.863	−2.923	−4.451	1.056	1.503
resting C_6 centered, carbon oriented	0.645	0.866	−2.922	−4.481	1.052	1.525
resting bond centered	0.380	0.184	−2.832	−4.323	1.110	1.706
resting carbon centered	0.346	0.251	−2.872	−4.434	1.149	1.731

iodine parameters. They fitted their dispersion parameters to the dispersion energies of Kochanski and Prissette;[23] used the repulsive parameters from the iodine−iodine force field of Rodger, Stone, and Tildesley;[36] and adjusted their point-charge representation to reproduce the main results of Kochanski and Prissette. We proceeded in a manner with fewer constraints, keeping our point-charge representation for iodine fixed, but varying our iodine−iodine interaction parameters to fit selected ab initio geometries.

The equilibrium geometries obtained from both sets of parameters are described in Table 7. As expected, since our ab initio geometries are similar to those of Kochanski and Prissette, our atom−atom potential derived geometry parameters are quite similar as well, differing from each other by at most 0.2 Å. The binding energies of our C_6-centered axial geometries are close as well (−3.28 kcal/mol vs −3.03 kcal/mol). However, our resting geometries are less tightly bound than Danten et al.'s resting geometries by almost 1 kcal/mol. This difference reflects the difference in the ab initio structures and binding energies chosen to derive the two atom−atom potentials. Since Kochanski and Prissette did not carry out calculations on resting structures, Danten et al.'s force field was fitted from axial structures only and is less likely to reproduce resting structure energies correctly.

It is instructive to examine the repulsive, dispersive, and electrostatic contributions to the binding energy of the geometries separately, as shown in Table 8. Danten et al. concluded that the dispersive interaction provided a relatively large and constant stabilizing energy to the complex, so that the relative energies of different conformations were determined by the balance of electrostatic and repulsive contributions. We reach essentially the same conclusion. The axial geometry is favored by electrostatics, while the resting geometry is favored by repulsive forces. Electrostatic and repulsive energies nearly cancel in the axial geometry; in the resting geometry, both energies are destabilizing. The dispersive energy is a practically constant −3 kcal/mol.

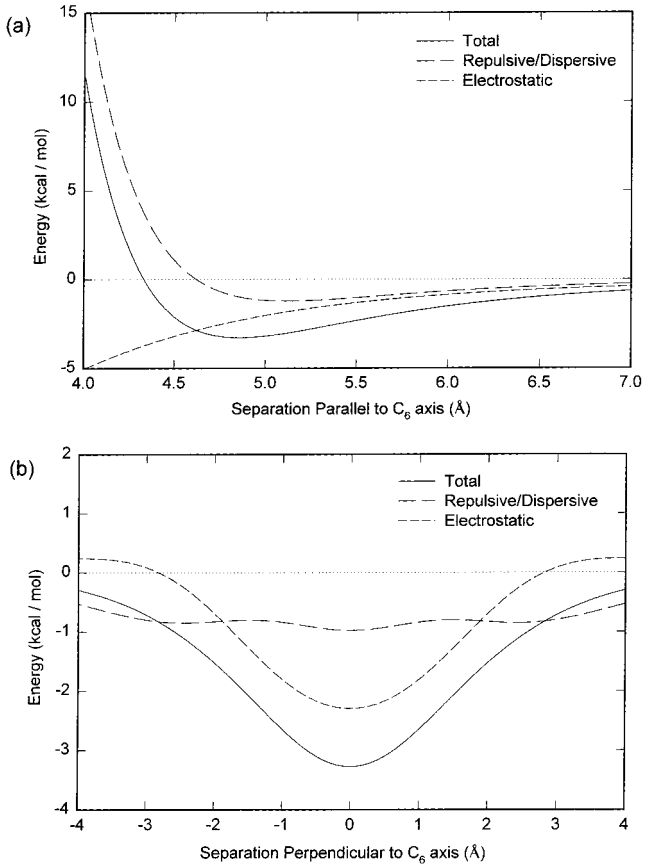

Figure 7. Potential energy surface of axial iodine moving (a) in and out of the benzene plane and (b) across the benzene plane. The energies are derived from the atom−atom potential fitted to ab initio results.

The magnitudes of the interactions, of course, differ. Consider the two minimum energy geometries examined by Danten et al.—the axial C_6 centered geometry and the resting bond-centered geometry. In Danten's study, the difference in the repulsive energies of the two geometries is less than 0.2 kcal/mol, and the most of the binding energy difference comes from the varying electrostatic interaction. In our study, the electrostatic energy varies almost identically, but an additional 1 kcal/mol difference in binding energy is obtained through a large repulsive interaction stabilization of the resting structure. This is the origin of the increased binding energy difference in our study.

It is also interesting to note where the differences in the binding energies of centered versus uncentered geometries arise. Potential energy surfaces of iodine moving both in and out of the benzene plane and across the benzene plane are shown in Figures 7 and 8. For the axial geometry, the repulsive and dispersive interactions nearly cancel across the benzene plane, so that the electrostatic interaction determines the location of axial structure minima. In our model, the result is that only one axial minimum is possible. This stands in contrast to our ab initio calculations, which indicate that the potential energy surface is actually much flatter, resulting in multiple axial minima.

In the case of the resting structure, the combined repulsive and dispersive interactions favor a central structure, but electrostatic interactions drive the iodine toward the edges of the benzene ring. The result is a nearly flat potential. Interestingly enough, the uncentered minimum energy structures have a noticeably lower binding energy because, by tilting a small amount, the repulsive and dispersive interactions acting on the

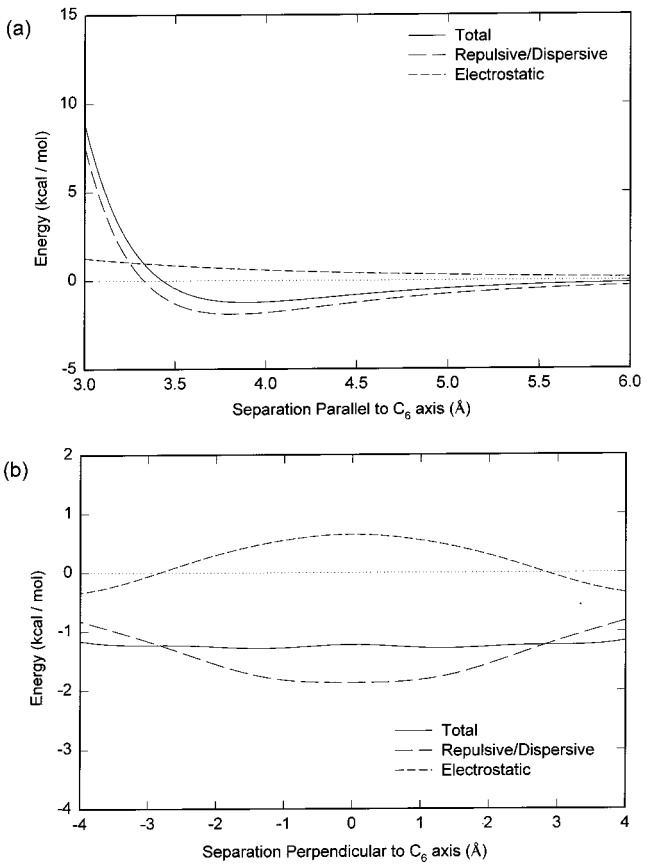

Figure 8. Potential energy surface of resting iodine moving (a) in and out of the benzene plane and (b) across the benzene plane. The energies are derived from the atom−atom potential fitted to ab initio results.

system may be strengthened without affecting the electrostatic contribution. This change in energy is enough to negate the variation of the combined repulsive and dispersive interactions across the benzene plane, so in the end, the relative binding energies of the off-centered minima are determined by the electrostatic interaction.

Once we have obtained an atom−atom potential description of the iodine−benzene complex, we may calculate the complex's heat of formation at a given temperature following the approach of Danten et al. We allow the iodine and benzene molecules to approach each other over the course of close to a million Monte Carlo steps. Out of these configurations, we average the binding energies of the complexes for which the center of mass separation is less than 6.5 Å. When this is done at 300 K, we find the average binding energy to be −0.85 kcal/mol, leading to a heat of formation of −1.44 kcal/mol. We note that without the 6.5 Å cutoff, we obtain a heat of formation of −1.24 kcal/mol.

Danten's calculations, in contrast, gives a heat of formation of −2.10 kcal/mol. Since our axial structure is bound more tightly than Danten's, this result indicates that although our resting structure is rather unstable, the complex is still spending a considerable portion of its time in that conformation. Indeed, because an axial iodine in our potential is drawn so strongly to the C_6 axis, there are many favorable resting configurations and only a few possible good axial configurations. If the potential energy surface for axial iodine moving across benzene was made flatter to better match the ab initio results, we would expect to see more axial configurations, with a corresponding increase in the magnitude of the complex's binding energy. This would bring our results closer to the experimental estimates of Atack and Rice[37] (−2.44 kcal/mol), Lang and Strong[38] (−2.0 kcal/mol), and Duerksen and Tamres[39] (−2.37 kcal/mol).

When studying large iodine−benzene clusters, it will be useful to compare the magnitude of the iodine−benzene interaction with that of the benzene-benzene interaction. The minimum energy structure of the benzene dimer using the Williams potential was found to have a structure between a parallel displaced configuration and a T-shaped configuration − one benzene was tilted about 30° away from parallel to the other. The structure has a binding energy of −2.64 kcal/mol, with an electrostatic contribution of −0.24 kcal/mol and a combined repulsive and dispersive contribution of −2.40 kcal/mol. In other words, 90% of the binding energy of the benzene dimer comes from dispersive + repulsive forces. The dispersive + repulsive forces make up only 30% of the binding energy of the axial iodine−benzene structure (Figure 7).

Minimum Energy 1:*n* Cluster Structures. We obtain from the Monte Carlo heating and quenching cycles 10 cluster geometries for each level of solvation. Superimposed atom positions of 1:1 and 1:2 iodine−benzene clusters are shown at both 30 and 200 K in Figure 9. At 30 K, all of the molecules are making small amplitude vibrations about their equilibrium positions. At 200 K, the molecules are no longer fixed and occasionally evaporate off the cluster.

The energies of the clusters thus obtained are plotted as a function of solvation level in Figure 10; corresponding lowest energy clusters for selected solvation levels are shown in Figure 11. Examining the energies of the lowest energy clusters, we find that the stabilization energy added by each new benzene rises from 3.3 kcal/mol for the first benzene to 8.2 kcal/mol for the 10th benzene. The electrostatic portion of this energy, however, remains relatively constant: the first benzene gives the system 2.3 kcal/mol stabilization, but each additional benzene typically gives 0.9 to 1.2 kcal/mol stabilization (aside from the first benzene, the maximum electrostatic stabilization is 1.8 kcal/mol).

As more and more benzenes are added, therefore, dispersive + repulsive interactions begin to dominate the stability provided by each new benzene. This fact is the key to explaining the next observation: that iodine is not generally located in the center of the benzene cluster. Instead, it prefers to stick *asymmetrically* out of one side of the cluster. There are two reasons for this. The first is that the benzene−benzene binding energy is smaller than the axial iodine−benzene binding energy but larger than the resting iodine−benzene binding energy. Therefore, once the sites at the ends of iodine are occupied, benzene would rather stick to other benzenes than it would to iodine.

The second reason is that electrostatic interactions provide 70% of the axial iodine−benzene binding energy (Figure 7). Once benzenes begin to surround one end of iodine, they shield the electrostatic interactions between benzene and iodine, causing the benzenes to stick to other benzenes instead of iodine. Additionally, since the benzene-benzene interaction is mostly dispersive in nature, the increased benzene surface area makes it especially favorable (both enthalpically and entropically) for the benzene molecules to cluster onto each other. This is why the dispersive + repulsive interaction energy dominates at high solvation ratios.

Molecular Reaction Dynamics. We have included snapshots from a typical iodine dissociation run in Figure 12. At 0 fs, the iodine molecule is bound in a somewhat oblique manner to the benzene below it. Three benzenes are bound directly to iodine, leaving two other benzenes to move freely over the

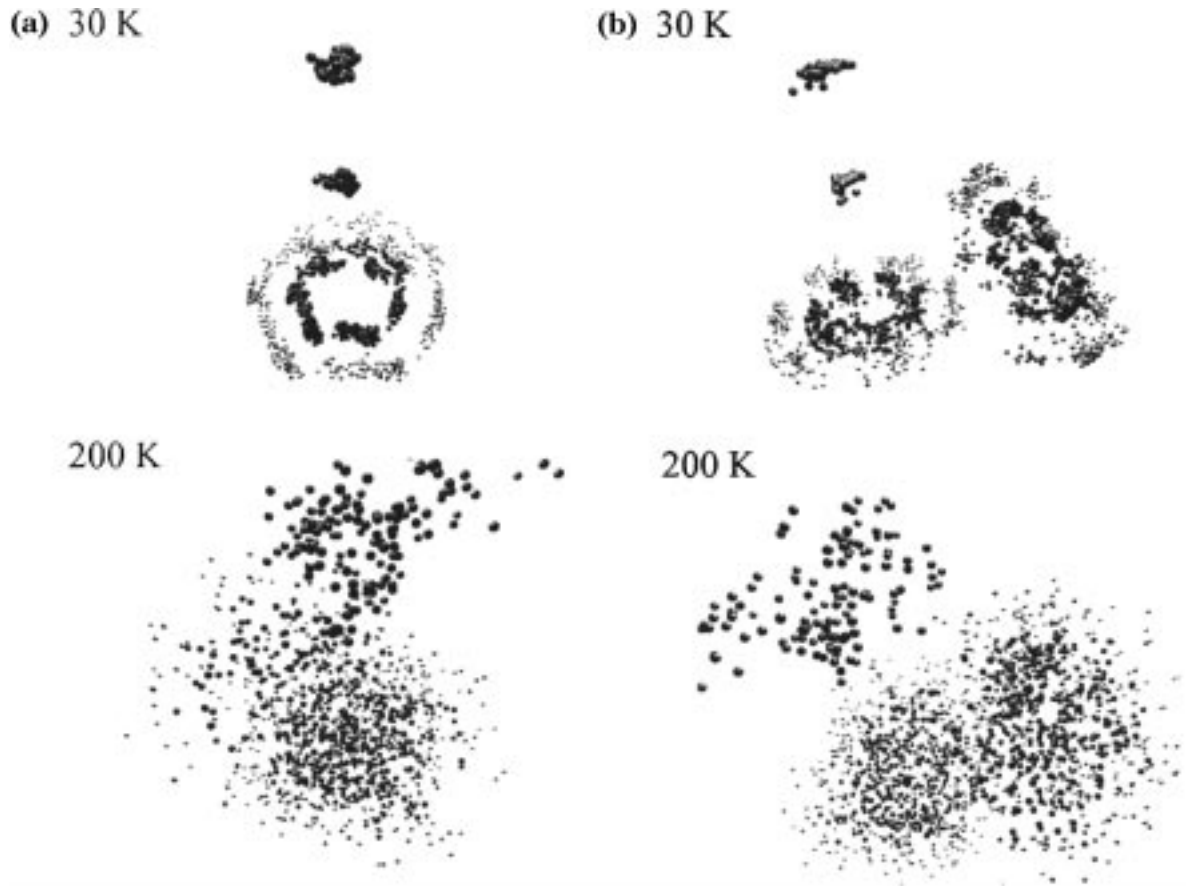

Figure 9. Superimposed nuclear positions of iodine−benzene clusters at 30 and 200 K over the first steps of a Monte Carlo run; (a) shows a 1:1 complex and (b) shows a 1:2 complex. The two iodine atoms are shown as the larger spheres on top of benzene (see the 30 K picture). The carbon and hydrogen atoms of benzene are represented by smaller black and gray spheres. The pattern is less clear at 200 K, but the iodine atoms still tend toward the upper portion of the plot.

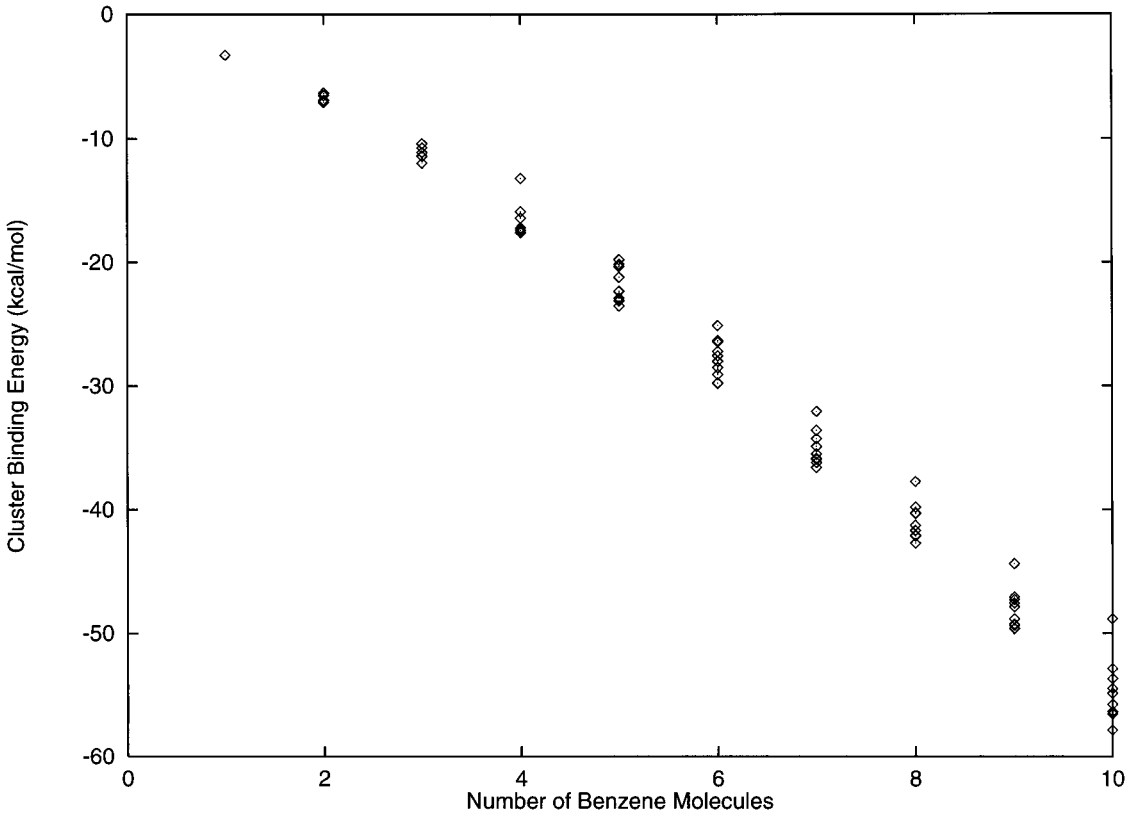

Figure 10. Energy of stable iodine−benzene clusters obtained from the Monte Carlo/quenching procedure as a function of solvation level.

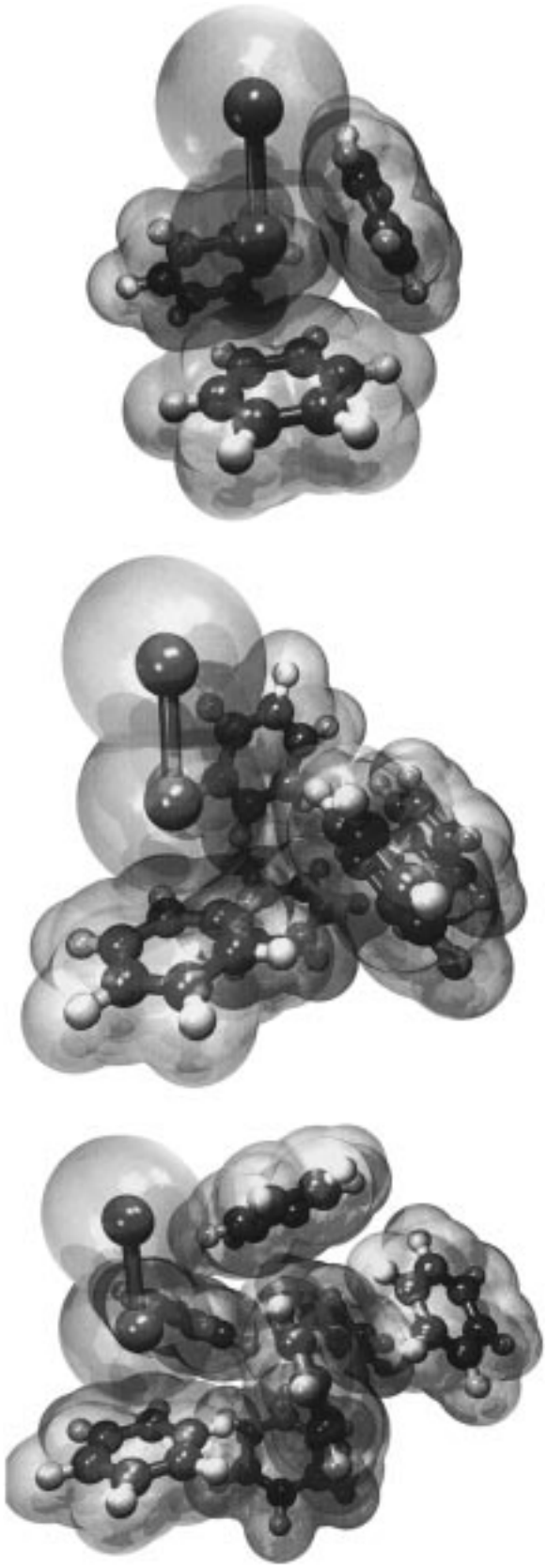

Figure 11. Minimum energy 1:*n* iodine−benzene clusters: (a) 1:3 complex, (b) 1:5 complex, (c) 1:7 complex.

surface of the benzene cluster. At 500 fs, the outward facing iodine has been partially ejected from the cluster but has not yet been detected. It does not leave the cluster in a straight line path, but curves around toward the center of the cluster, dragging it along as it does so. At 1000 fs (not shown), the benzene that the iodine molecule was originally resting on has started to leave the cluster, and after 2000 fs, both a single iodine atom and a single benzene molecule have been ejected. At around this point, the ejected iodine atom is sufficiently far enough away from the cluster to be detected. The second iodine atom is caged by the remaining benzene molecules and will leave the cluster after a few tens of picoseconds.

In observing caging dynamics, we are primarily interested in seeing how long an iodine atom remains next to any benzene molecule. We have examined this process in Figure 13, where the distance between each iodine atom and the benzene molecule closest to it is plotted over time for 25 superimposed trajectories. Iodine atoms are assumed to be detectable once they are at least 10 Å away from all benzene molecules. The detection threshold is represented by a dotted line on these graphs.

We would expect the 1:1 complexes studied to be in a close to axial geometry. The trajectories thus observed reflect this: half the iodine atoms are initially pointing away from the benzene molecule, and leave within half a picosecond; the other half collide with and are slowed by the adjacent benzene. They leave within one and a half picoseconds. Two classes of iodine atoms with different caging rates and kinetic energies are therefore present. Note that the iodine atoms facing toward the benzene leave with a wider range of kinetic energies than the other iodine atoms, due to the range of impact geometries present.

Higher solvation ratios produce similar results. The asymmetry of the complex produces two classes of iodine atoms: ones initially pointing out of the complex, and ones pointing into the complex. The ones pointing outward leave quickly, within a few picoseconds. This first caging time increases with increasing solvation, since the escaping iodine atom transfers some of its momentum to nearby benzene molecules by dragging them along, and so having more benzene molecules nearby slows down the iodine. The iodine atom facing the complex is ejected into the cluster of benzenes with high kinetic energy. This increases the vibrational energy of the cluster, often leading to the ejection of more weakly bound benzene molecules. The iodine atom, however, often loses enough energy immediately to the benzenes that it is not immediately ejected. Caging has occurred. At a time scale, typically in the tens of picoseconds, that depends on the vibrational energy of the cluster, the trapped iodine atom will migrate away from the center of the cluster and be ejected. As with the first caging time, the second caging time increases with increasing solvation ratio.

We have hypothesized that the two classes of iodine atoms, separated by caging time and kinetic energy, observed experimentally are the result of the asymmetric nature of the iodine−benzene clusters. Therefore, we predict that an iodine molecule, when dissociated, splits into two iodine atoms, each of which is in a different class. If one atom is caged, the other is released immediately, and vice versa. It is possible to imagine situations where this is not the case. For example, suppose we start with a collection of benzene clusters and an equal number of iodine molecules. Then, suppose half the iodine molecules integrate themselves into the center of half the benzene clusters. Upon dissociation, two classes of iodine atoms corresponding to the associated and nonassociated iodine molecules would be formed.

To verify our original hypothesis, then, we must do more than simply verify the existence of two classes of iodine molecules. We must show that the caging times of bound iodine atoms are *correlated*. To do this, for each trajectory we take the two iodine atoms in the iodine molecule, call them I_1 and I_2, and plot the minimum iodine atom to benzene distances

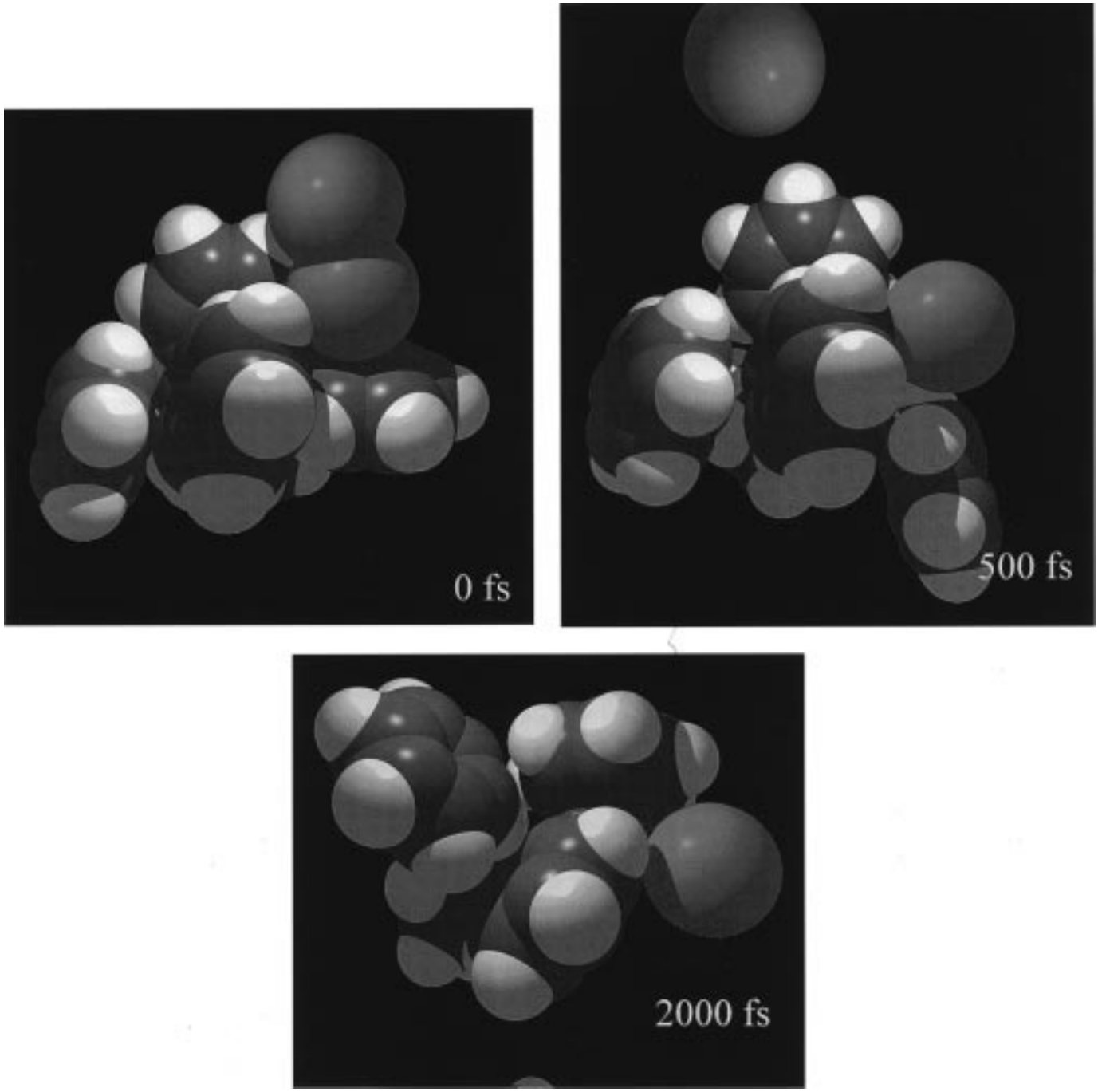

Figure 12. Snapshots from a typical iodine dissociation molecular dynamics run with five benzenes at, (top left) 0 fs, (top right) 500 fs, and (bottom) 2000 fs, showing the release of a fast-rise iodine atom and the subsequent caging of a slow-rise iodine atom.

$D(\mathrm{Bz-I_1})$ and $D(\mathrm{Bz-I_2})$ against each other over time, as shown in Figure 14. We then expect to see trajectories running along the axes of the parametric plot, indicating that only one atom per trajectory is caged. And this is indeed what we observe. For the 1:1 solvation ratio, no atoms are truly caged; there are not enough benzenes to dissipate the iodine atoms' kinetic energy. But we clearly observe that when one atom leaves quickly, the other leaves slowly. Sometimes both atoms leave at the same speed, so that they do not fall into separate classes. As the solvation ratio increases, the iodine atoms in the clusters are more likely to be solvated equally and more "diagonal trajectories", showing the release of the two atoms with the same speed, become evident (see Figure 14).

Finally, we would like to reproduce time-of-flight mass spectrometry (TOFMS) data obtained by Cheng et al.[4] that describes how the number of free iodine atoms observed after the induced dissociation of I_2 varies with time. To do this, we use the detection threshold of 10 Å mentioned above, and in Figure 15 we plot the number of free iodine atoms over time averaged over a large number of trajectories.

In the TOFMS experiments, transients are obtained over a wide range of cluster size distributions. Figure 16 shows a range of molecular beam cluster compositions and their corresponding TOFMS transients. Since it is not clear that benzene clusters of differing sizes are ionized and detected in the same way, the cluster compositions shown in the figures must be regarded as a rough representation of the actual cluster size distribution. Because of this uncertainty, we do not expect our theoretically obtained caging time scales to directly match the time constants fit and shown in Figure 16.

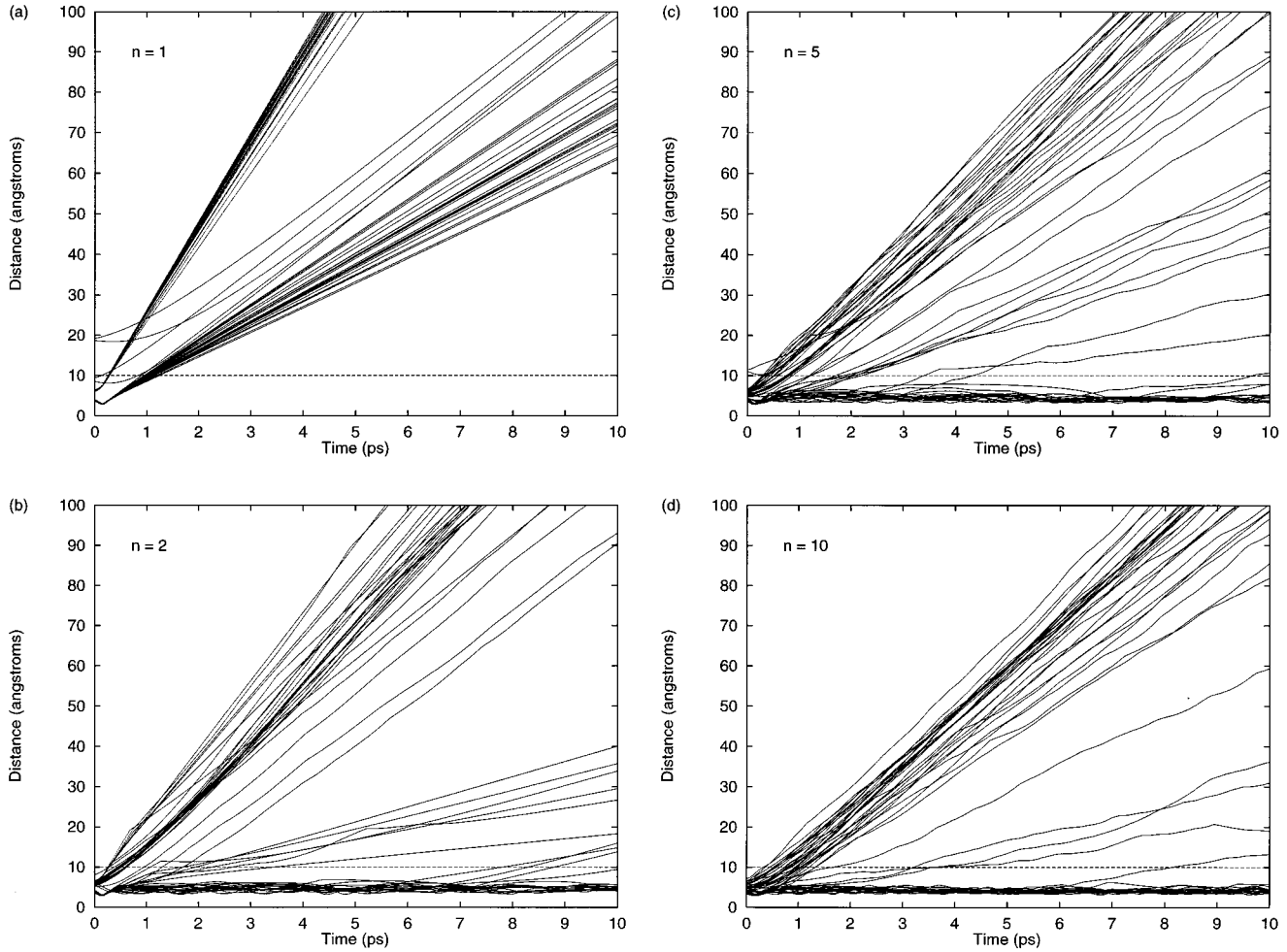

Figure 13. The variation of the distance between each iodine atom and the benzene molecule closest to it over the first 10 ps following iodine dissociation. A plot of twenty-five superimposed trajectories are shown for (a) the 1:1 complex, (b) the 1:2 complex, (c) the 1:5 complex, and (d) the 1:10 complex.

TABLE 9: Time Constants from the Simulated Transients Shown in Figure 15[a]

solvation ratio	τ_1 (ps)	τ_2 (ps)
1:1 I_2−Bz	0.66[b]	N/A
1:2 I_2−Bz	0.82	90
1:5 I_2−Bz	1.08	65
1:10 I_2−Bz	1.17	200

[a] Data from the 1:1 complex was fit to a single-exponential curve; data from the 1:2, 1:5, and 1:10 clusters were fit to biexponential curves. [b] Since the fit is over 50 ps, there is no resolution of the two types of trajectories involved (see Conclusion section).

For the most part, as detailed in Table 9, the simulated transients of Figure 15 show a clear biexponential behavior with both time scales increasing with increased solvation ratios. The only exception is an apparent reversal of the slow caging time constant of the 1:2 and 1:5 iodine−benzene clusters. This anomaly is almost certainly caused by not having enough trajectory data and further calculations are needed.

We find that the experimental fast caging times range from 0.75 to 2.3 ps; the corresponding theoretical times range from 0.66 to 1.17 ps. The slow caging times range from 19 to 75 ps experimentally; theoretically, the slow caging times range from 90 to 200 ps. In other words, experimental results show that the benzene cluster holds the first iodine atom to leave more tightly than expected, and holds the second iodine atom to leave *less* tightly than expected. This discrepancy may suggest that the solvation shell around the iodine molecule is not as asymmetric as calculated and/or the cluster potentials need modification.

As mentioned previously, the binding of benzenes to each other is governed by dispersive + repulsive forces, but the binding of benzene to iodine is essentially driven by electrostatics (Figure 7). That asymmetric clusters form is a consequence of the intrinsic disparity of these interactions. The shape that the benzene cluster assumes as it draws around iodine, however, is determined by an interplay between the charge distribution on the benzene cluster surface and the electrostatics of iodine. This interaction is significantly more difficult to approximate via a simple atom−atom potential.

For instance, although iodine is highly polarizable, we have assumed that the binding of benzene does not cause any changes in its charge distribution. This is in fact untrue. Benzenes binding around one end of iodine cause charge to be drawn away from iodine's bond midpoint, making it easier for additional benzenes to bind there. This effect is especially significant in the cavity where iodine is folded into benzene. Iodine's polarization is therefore expected to "stretch" the benzene cluster out toward the outfacing end of iodine, causing the outward iodine atom to be bound more tightly and allowing the inward iodine atom to more readily escape.

In this way, we see that although our model can successfully predict zeroth order structural features—that the iodine−benzene cluster is asymmetric—it falls short of predicting first-order features—the exact degree of this asymmetry. The model may

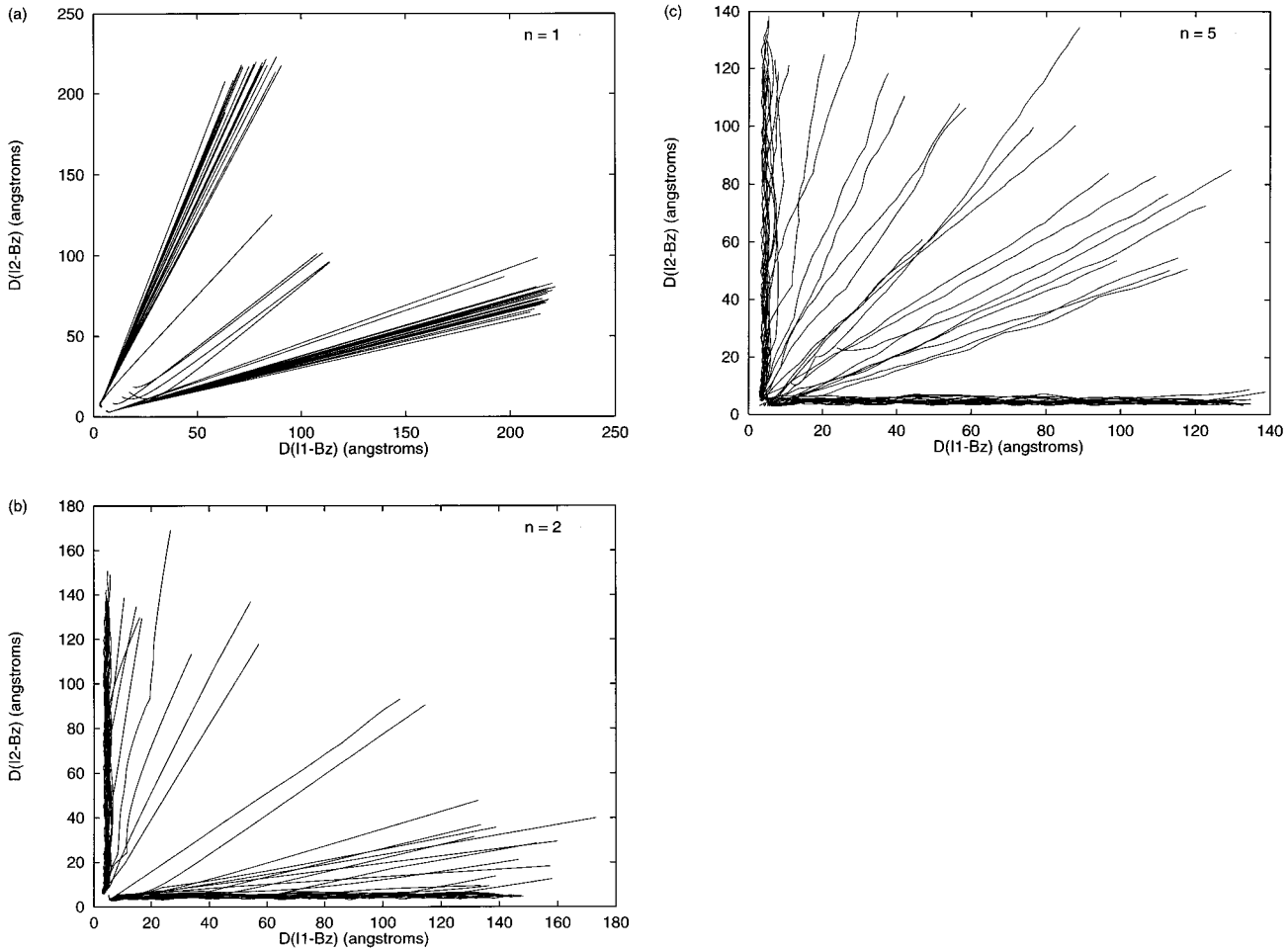

Figure 14. Correlation of the trajectories of previously bound iodine atoms I_1 and I_2. A parametric plot of the minimum iodine−benzene atom distances $D(\mathrm{Bz}-\mathrm{I}_1)$ and $D(\mathrm{Bz}-\mathrm{I}_2)$ is shown over time for (a) the 1:1 complex, (b) the 1:2 complex, and (c) the 1:5 complex.

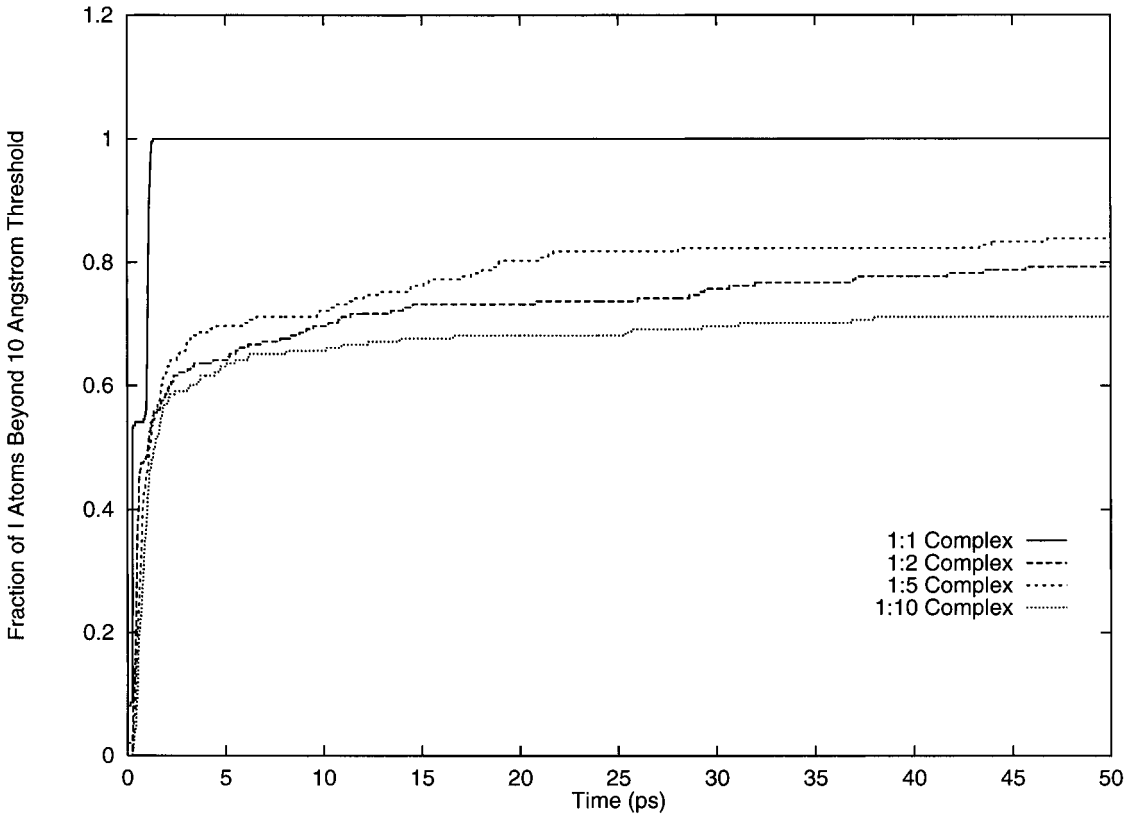

Figure 15. The number of free iodine atoms over time is plotted from the averaged trajectories of molecular dynamics simulations. Note the distinct femtosecond and picosecond time scales.

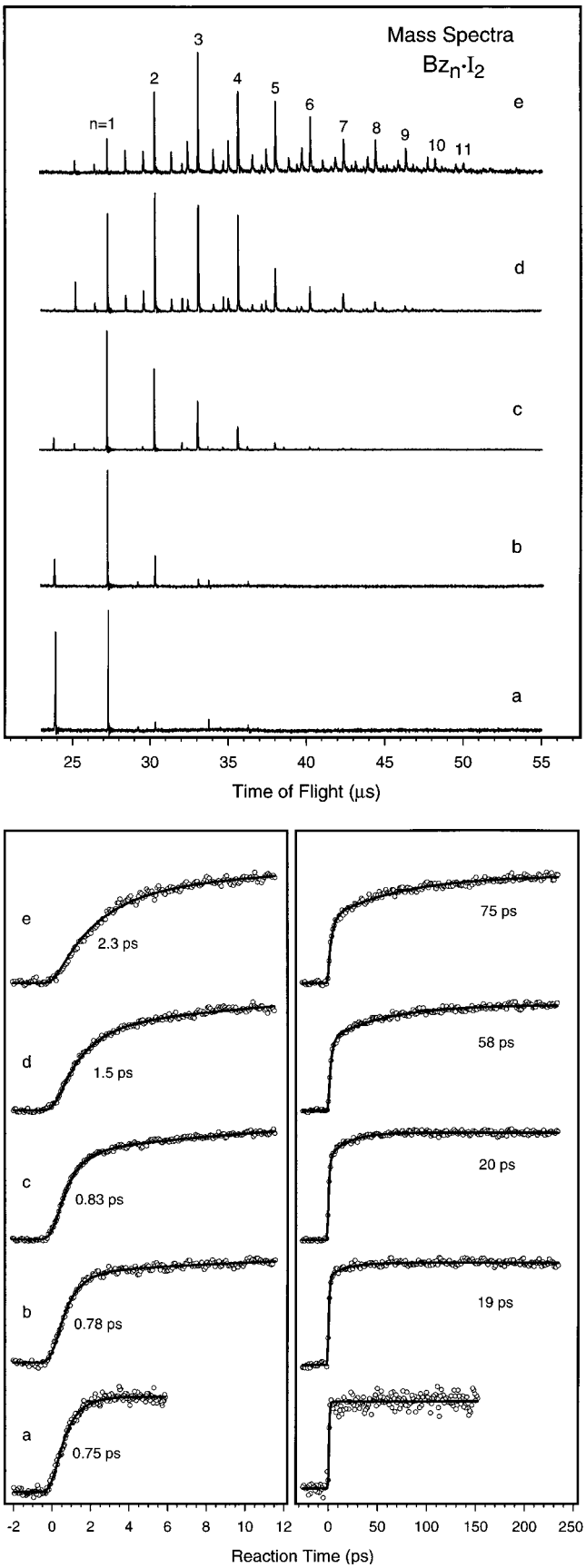

Figure 16. Experimental results from Cheng et al.[4] showing (top) the variation of iodine−benzene cluster size in the molecular beam as a function of benzene vapor pressure (a−e) and (bottom) TOFMS transients for the cluster distributions indicated in the top figure).

be improved by incorporating many body effects into the solvation process via a consideration of iodine polarizablity, or by adjusting the charge distribution on iodine with increasing solvation to account for these effects in an average manner. In the latter case, experimental caging times may be used to guide the selection of parameters describing iodine's charge distribution. Alternatively, further work could consider the full quantum structural determination of larger iodine−benzene clusters.

IV. Conclusion

In this contribution, we have examined the process of iodine dissociation reactions in benzene clusters. Experimentally, it has been noted that this process leads to the ejection of iodine atoms from the cluster on two different time scales. We have hypothesized that this effect arises from a basic asymmetry in the structure of the complex. This hypothesis has been confirmed theoretically using ab initio, Monte Carlo, and molecular dynamics simulations. The results illustrate that caging experiments can provide fundamental insights into the structural features of solvation.

More specifically, the main conclusions of this work are as follows: First, iodine may lie near-axially to benzene with a binding energy of −3.5 kcal/mol or may lie flat on benzene with a binding energy of −1.7 kcal/mol. In both cases, the iodine is highly mobile, and moves across the benzene ring freely, hindered only by an energy barrier no higher than 0.5 kcal/mol.

Second, when the ab initio calculations of electrostatic potential and energies are used to deduce the atom−atom potentials, we find that 70% of the binding energy of the axial 1:1 complex is due to electrostatic forces and that the remaining 30% is due to combined dispersive and repulsive forces. The atom−atom potential reproduces the structures and energies of the centered geometries (from which the potential was derived) well. In the resting case, the potential energy surface across benzene is flat, but in the axial case the potential energy surface strongly favors a central position for iodine. The ab initio calculations indicate a much flatter potential energy surface for axially oriented iodine moving across benzene.

Third, iodine−benzene clusters are *asymmetric*. Benzene molecules would rather cluster around each other than around iodine, so iodine tends to stick out of one end of the cluster. The benzenes arrange themselves into a "mouth-like" formation, or equivalently, the iodine is partially "immiscible" in benzene.

Fourth, the two classes of caged iodine atoms, different in both caging times and kinetic energies, is created by the asymmetry of the structure. One iodine atom is pointed into the cluster, while the other iodine atom points away from the cluster. When the iodine bond is broken, the iodine atom facing away from the cluster flies away rapidly and is detected within a few picoseconds. Its caging time is determined by the size of the cluster it transiently drags along as it leaves. The other iodine atom is absorbed into the cluster, and is released on a time scale dependent on the vibrational energy of the cluster. When one atom is released immediately, the other tends to be caged. Trajectory calculations for the 1:1 complex show two time scales for the "free" and "caged" atoms (see Figures 13a and 16); the experimental 0.75 ps rise (a) in Figure 16 is actually made of two components (0.4 and 1.4 ps)[4] consistent with the calculations. For larger clusters, two types of trajectories, free and caged, were clearly dominant.

Finally, the caging time scales of both iodine atoms increase steadily with increasing solvation ratio. This is in agreement with experiment. The exact difference in fast and slow caging times, which is dependent on the cluster's degree of asymmetry, is less well predicted, and future studies of the complex using

more complex potentials or quantum calculations of larger clusters may better quantify these time scales. The solvation structures obtained here are reminiscent of those found in studies of iodine in large argon clusters by Martens' group[40] and of hydrogen fluoride in small argon clusters studied by Schinke, Bačić, and colleagues.[41] However, as described above, the unique predominance of dispersive + repulsive interactions between benzenes and electrostatic interactions between iodine and benzene is critical to the structure and dynamics of the benzene solvent cage around iodine.

Acknowledgment. This work was supported by the National Science Foundation. J. Su wishes to thank the SURF program and T. Tombrello of the Ph 11 course at Caltech for summer fellowships. We also thank V. McKoy, W. Goddard, K. Kuwata, P. Cheng, S. Baskin, and E. Diau for their help and suggestions. We thank Dongping Zhong and the referees for their thorough reading of the manuscript and for their useful comments.

References and Notes

(1) Mulliken, R. S. *J. Am. Chem. Soc.* **1950**, *72*, 610.
(2) Lenderink, E.; Duppen, K.; Everdij, F. P. X.; Marvi, J,; Torre, R.; Wiersma, D. A. *J. Phys. Chem.* 1996, *100*, 7822.
(3) Zewail, A. H. In *Femtochemistry and Femtobiology*; Sundstrom, V., Ed. World Scientific: Singapore, 1998.
(4) Cheng, P. Y.; Zhong, D.; Zewail, A. H. *J. Chem. Phys*. **1996**, *105*, 6216.
(5) Cheng, P. Y.; Zhong, D.; Zewail, A. H. *J. Phys. Chem.* **1995**, *99*, 15733.
(6) Collin, J.; D'Or, L. *J. Chem. Phys.* **1955**, *23*, 397.
(7) Yarwood, J.; Person, W. B. *J. Am. Chem. Soc.* **1968**, *90*, 594.
(8) Mulliken, R. S. *J. Chem. Phys.* **1955**, *23*, 397.
(9) Ferguson, E. E. *J. Chem. Phys.* **1956**, *25*, 577.
(10) Fredin, L.; Nelander, B. *J. Am. Chem. Soc.* **1974**, *96*, 1672.
(11) Hassel, O.; Stromme, K. O. *Acta Chem. Scand.* **1959**, *13*, 1781.
(12) Hassel, O.; Stromme, K. O. *Acta Chem. Scand.* **1958**, *12*, 1146.
(13) Mulliken, R. S.; Person, W. B. *Molecular Complexes: a Lecture and Reprint Volume*; Wiley-Interscience: New York, 1969.
(14) Lippert, J. L.; Hanna, M. W.; Trotter, P. J. *J. Am. Chem. Soc.* **1969**, *91*, 4035.
(15) Cook, E. G.; Schug, J. C. *J. Chem. Phys* **1970**, *53*, 723.
(16) Schug, J. C.; Dyson, M. C. *J. Chem. Phys* **1973**, *58*, 297.
(17) Mulliken, R. S. *J. Chem. Phys* **1965**, *43*, S2.
(18) Stone, A. J. *Chem. Phys. Lett.* **1993**, *211*, 101.
(19) Schug, J. C.; Levinson, K. A. *Theor. Chim. Acta* **1975**, *37*, 269.
(20) Bruns, R. E. *J. Molecular Structure* **1977**, *36*, 121.
(21) Jano, I. *Theor. Chim. Acta* **1985**, *66*, 341.
(22) Lucchese, R. R.; Schaefer, H. F. *J. Am. Chem. Soc.* **1975**, *97*, 7205.
(23) Kochanski, E.; Prissette, J. *Nouv. J. Chimie* **1980**, *4*, 509.
(24) Everdij, F. P. X.; van der Spoel, D.; Mavri, J.; Wiersma, D. A. In *Femtochemistry and Femtobiology*; Sundstrom, V. Ed.; World Scientific: Singapore; 1998. Also personal communication.
(25) Danovich, D.; Hrusak, J.; Shaik, S. *Chem. Phys. Lett.* **1995**, *233*, 249.
(26) Lin, Z.; Hall, M. B. *Polyhedron* **1993**, *12*, 1499.
(27) Hu, W.; Truhlar, D. G. *J. Phys. Chem.* **1994**, *98*, 1049.
(28) Oberle, C.; Eysel, H. H. *J. Mol. Struct. (THEOCHEM)* **1993**, *280*, 107.
(29) Setokuchi, O.; Shimizu, Y. *J. Mol. Struct. (THEOCHEM)* **1993**, *281*, 67.
(30) Frisch, M. J.; Trucks, G. W.; Head-Gordon, M.; Gill, P. M. W.; Wong, M. W.; Foresman, J. B.; Johnson, B. G.; Schlegel, H. B.; Robb, M. A.; Replogle, E. S.; Gomperts, R.; Andres, J. L.; Raghavachari, K.; Binkley, J. S.; Gonzales, C.; Martin, R. L.; Fox, D. J.; Defrees, D. J.; Baker, J.; Stewart, J. J. P.; Pople, J. A. *Gaussian 92* Gaussian, Inc.: Pittsburgh, PA.
(31) Potter, D. *Comput. Phys.* Wiley: New York; 1972.
(32) Chalasinski, G.; Szczesniak, M. M. *Chem. Rev.* **1994**, *94*, 1723.
(33) Hobza, P.; Selzle, H. L.; Schlag, E. W. *Chem. Rev.* **1994,** *94*, 1767.
(34) Danten, Y.; Guillot, B.; Guissani, Y. *J. Chem. Phys.* **1991**, *96*, 3782.
(35) Straub, P. A.; McLean, A. D. *Theor. Chim. Acta* **1974**, *32*, 227.
(36) Rodger, P. M.; Stone, A. J.; Tildesley, D. J. *Chem. Phys. Lett.* **1988**, *145*, 365.
(37) Atack, D.; Rice, O. K. *J. Phys. Chem.* **1954**, *58*, 1017.
(38) Lang, F. T.; Strong, R. L. *J. Am. Chem. Soc.* **1965**, *87*, 2345.
(39) Duerksen, W. K.; Tamres, M. *J. Am. Chem. Soc.* **1968**, *90*, 1379.
(40) Martens, C. G. In *Femtochemistry*; Chergui, M. Ed.; World Scientific: Singapore; 1996.
(41) Schröder, T.; Schinke, R.; Liu, S., Bačić, Z.; Moskowitz, J. W. *J. Chem. Phys.* **1995**, *103*, 9228.